PPPL Mini Space Physics Workshop, Aug. 2004

Opening of Magnetic Fields in Coronal Mass Ejections

G. S. Choe

Princeton Plasma Physics Laboratory
Princeton University
Princeton, NJ 08543-0451

Progress of a Coronal Mass Ejection

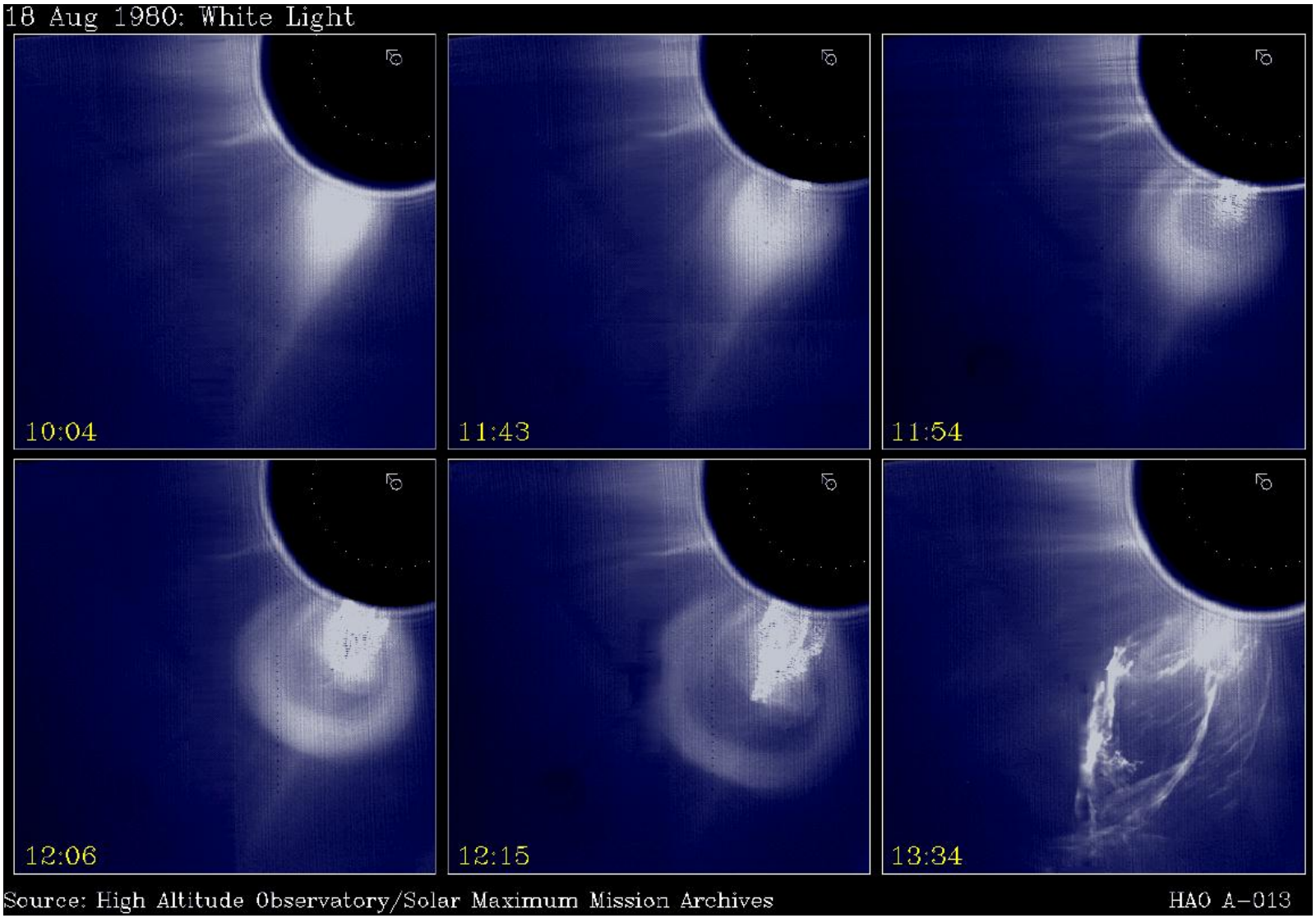

Physical Parameters of CMEs

- Speed: $10-2{,}000\,\mathrm{km\,s^{-1}}$ $(500\,\mathrm{km\,s^{-1}})$
- Mass: $10^{14}-10^{17}$ g $(10^{15}$ g$)$
- Kinetic Energy: $10^{28}-10^{33}$ erg $(10^{30}$ erg$)$

Numbers in the parentheses are for the event shown in the previous slide (1980/08/18).

Field Opening in a CME

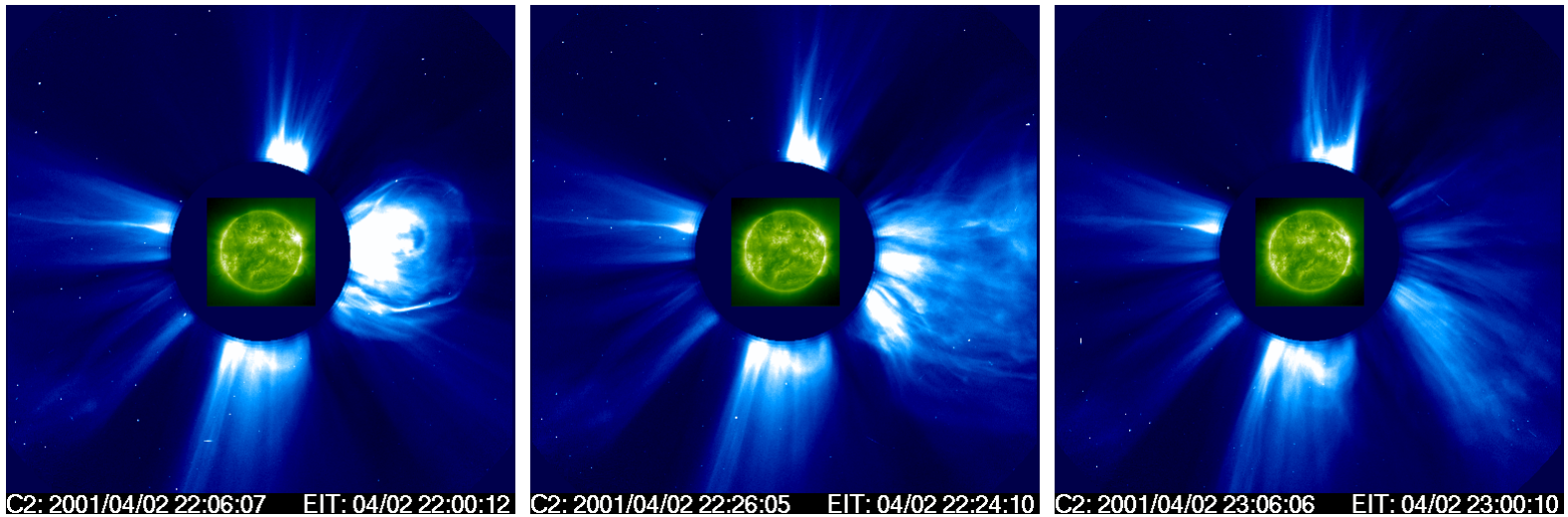

LASCO C2 and EIT composite images showing the evolution of the CME that took place on 2001/04/02

LASCO C2 Movie of the CME on 2001/04/02

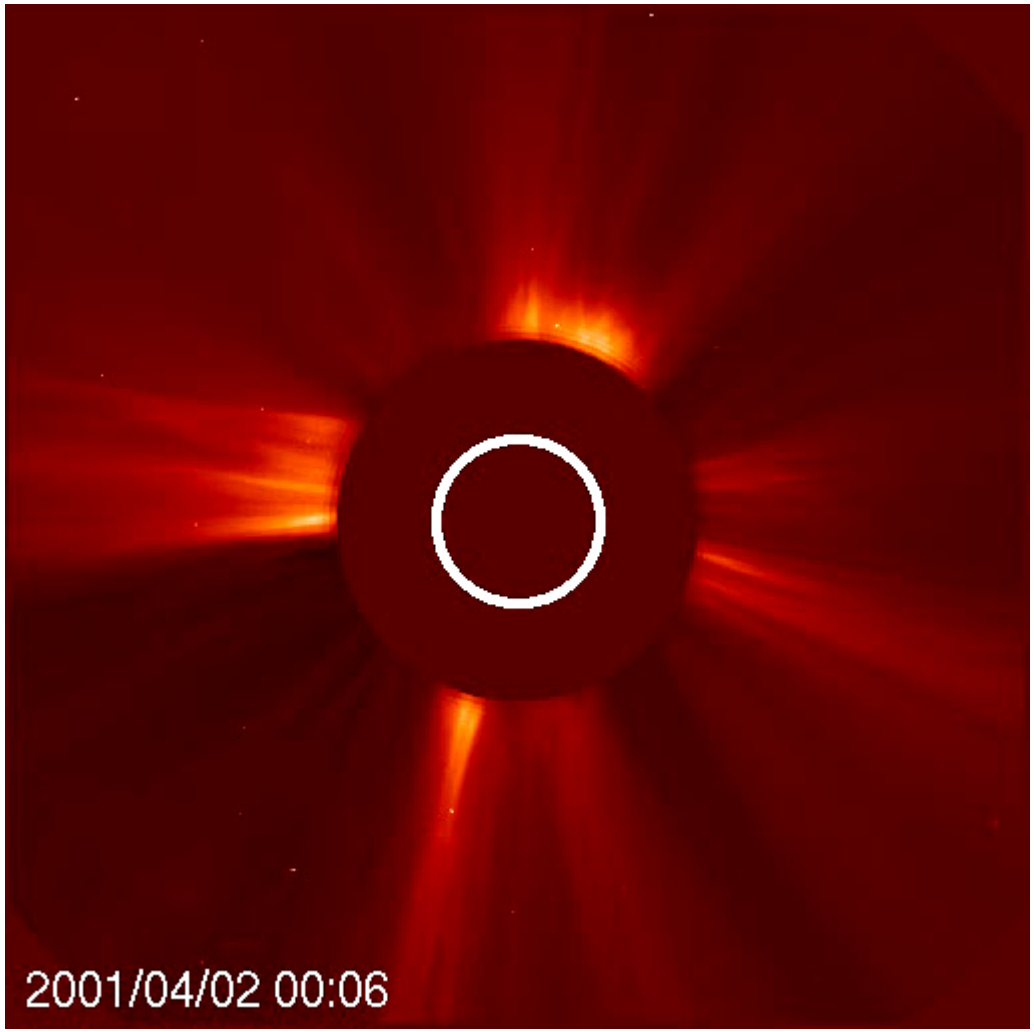

Sketch of Observed CME Progress

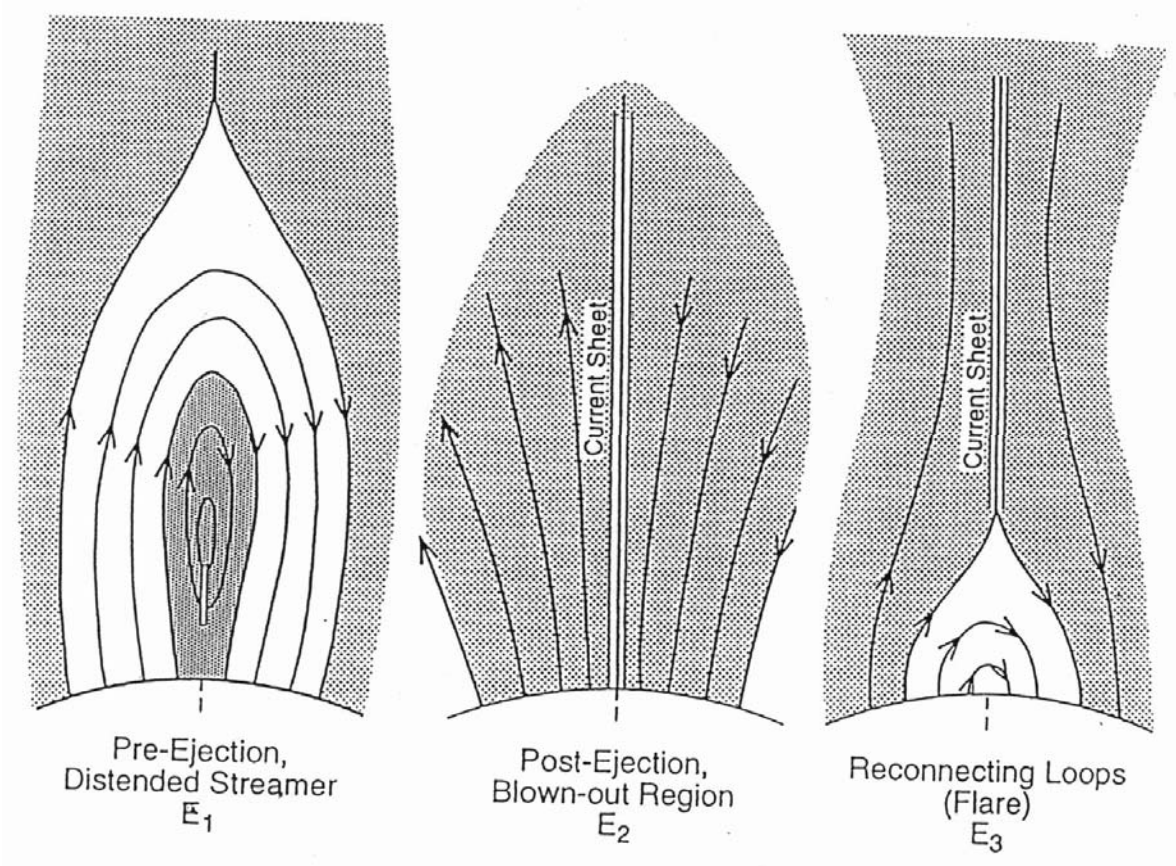

$E_1 > E_2$? $E_2 > E_3$ natural

On the Field Opening

- Observations indicate:
  - Field opening may be **partial**, but considerable part of the whole flux opens up.
  - Field opening must be a **spontaneous, energy-releasing** process.
- We naturally raise the question:

$$E_{\text{closed}} > E_{\text{open}} \ ?$$

- As for force-free fields,
  <u>Aly-Sturrock theorem</u> says **No !**

Aly-Sturrock Theorem

In an infinite space outside a certain boundary, the least upper bound of energy of force-free fields, whose lines of force are unknotted and connected to the boundary, and which have the same boundary normal field distribution, is the energy of the corresponding open field.

$$E_{\text{potential}} \leq E_{\text{fff}} \leq E_{\text{open}}$$

Theories of CMEs

Since Aly's conjecture, CME theories have tried to get around the idea of field opening as a spontaneous energy-releasing process.

- Partial opening without energy release
- Virtual opening by magnetic reconnection
  - 'Magnetic breakout'
- Catastrophe in flux rope equilibrium
- Current driven instability of flux ropes
- Ejection of self-closed field structures

Partial Opening w/o Energy Release

(Mikic & Linker 1994, Roumeliotis et al. 1994, Amari et al. 1996)

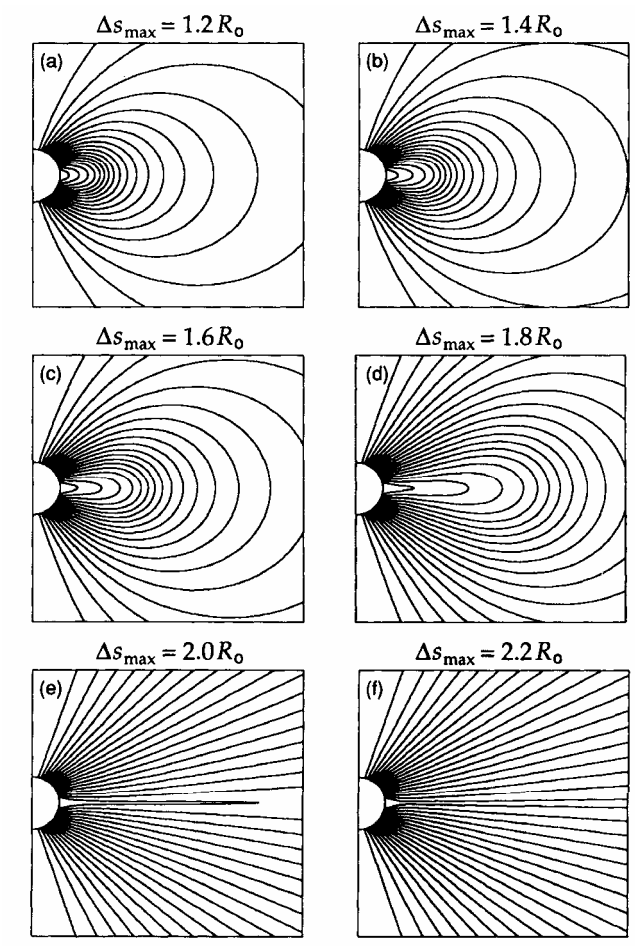

$\beta = 0$ (force - free)

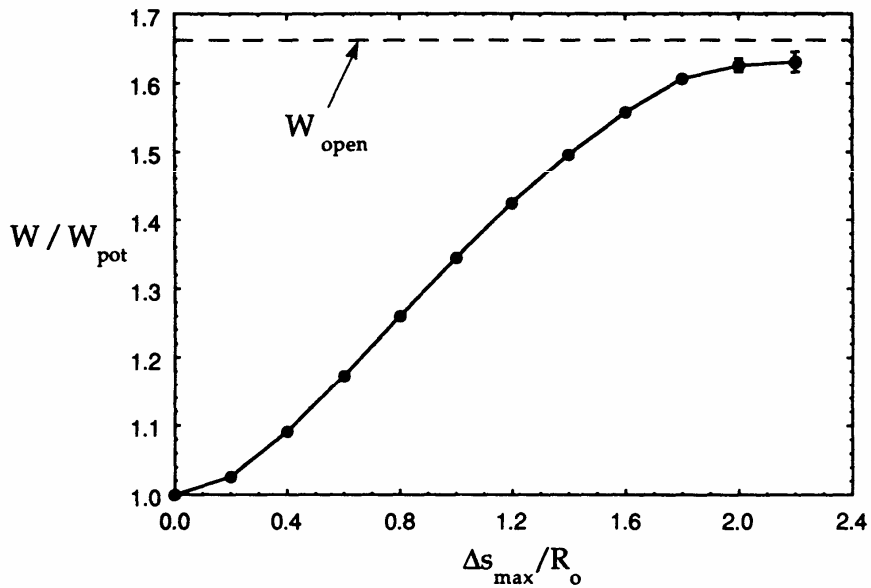

Mikic & Linker 1994

Problems in Models of Partial Opening w/o Energy Release

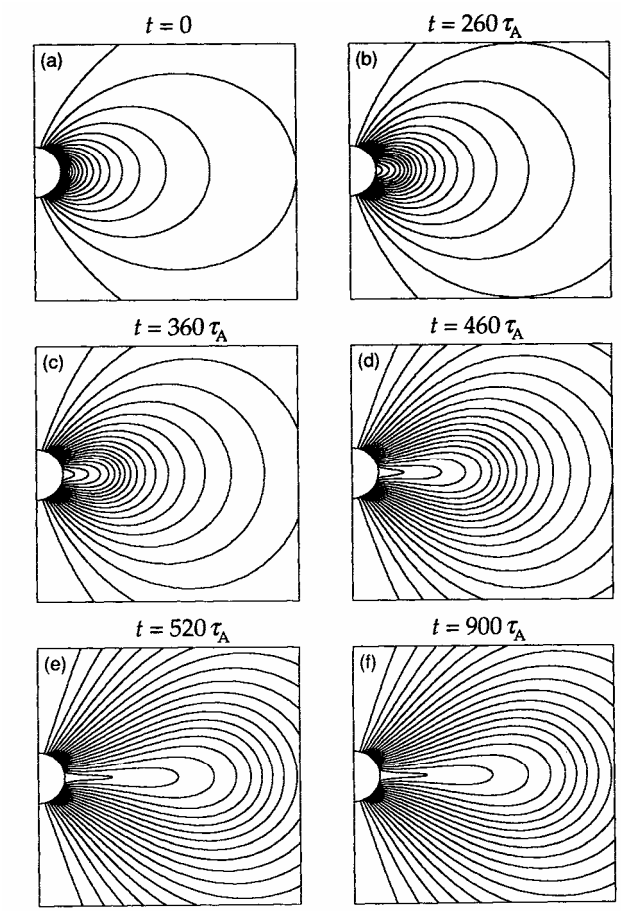

$\beta \approx 0.05$

- No field opening for non-force-free fields, even for very low beta.
- No energy is available for mass expulsion in CMEs.

Magnetic Breakout – Virtual Opening

(Antiochos 1998, 1999)

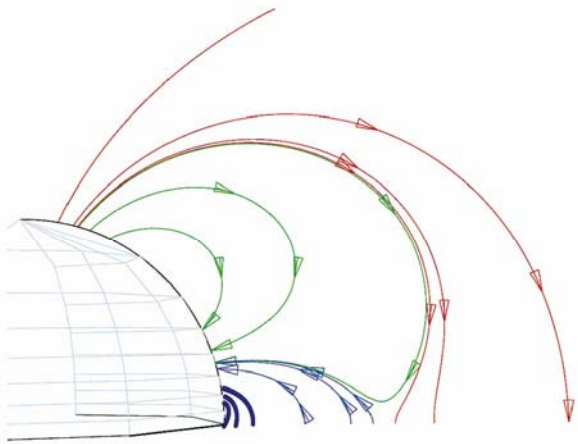

FIG. 4*a*

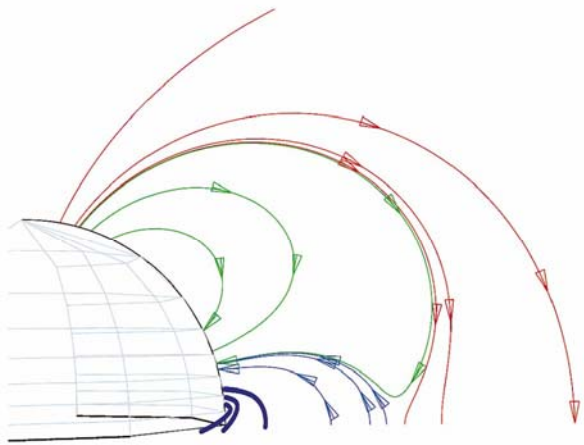

FIG. 4*b*

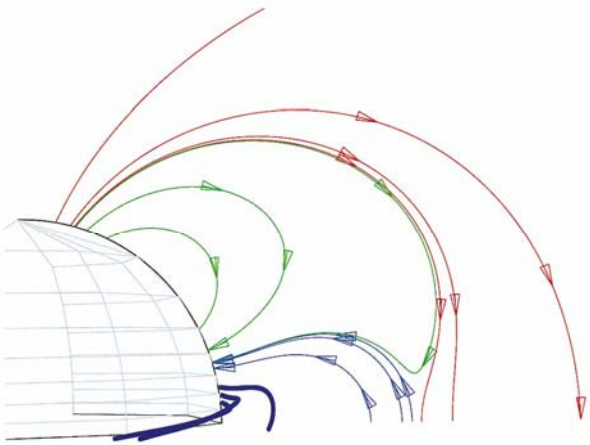

FIG. 4*c*

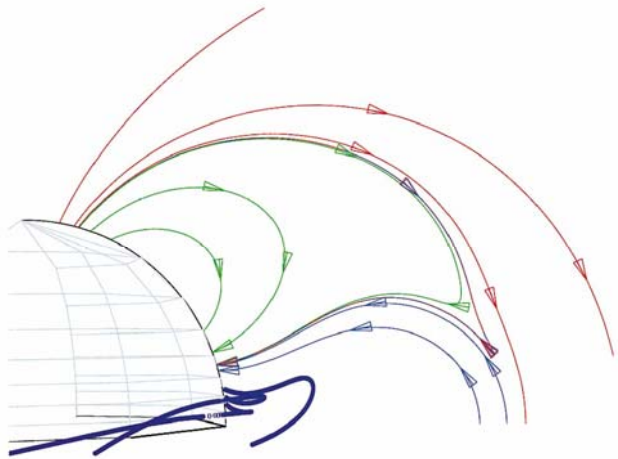

FIG. 4*d*

Comments on the Breakout Model

- The underlying flux must be more than the overlying flux and all the overlying flux must be reconnected.

- The model itself does not provide explanation of flaring processes. The most plausible flaring scenario is nothing else than the CSHKP model.

Flux Rope Catastrophe Model

(Van Tend, Kuperus, Forbes, Priest, Isenberg, Lin)

Assumption

- The solar surface is a rigid perfect conductor.
- Thus, the coronal current is closed on the photosphere.

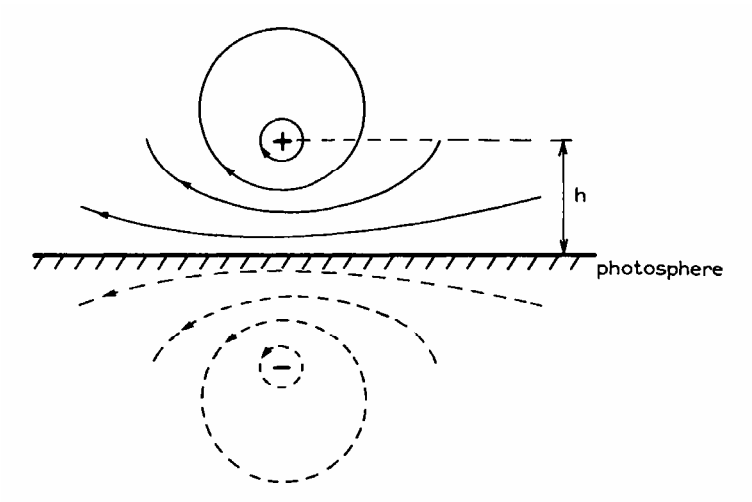

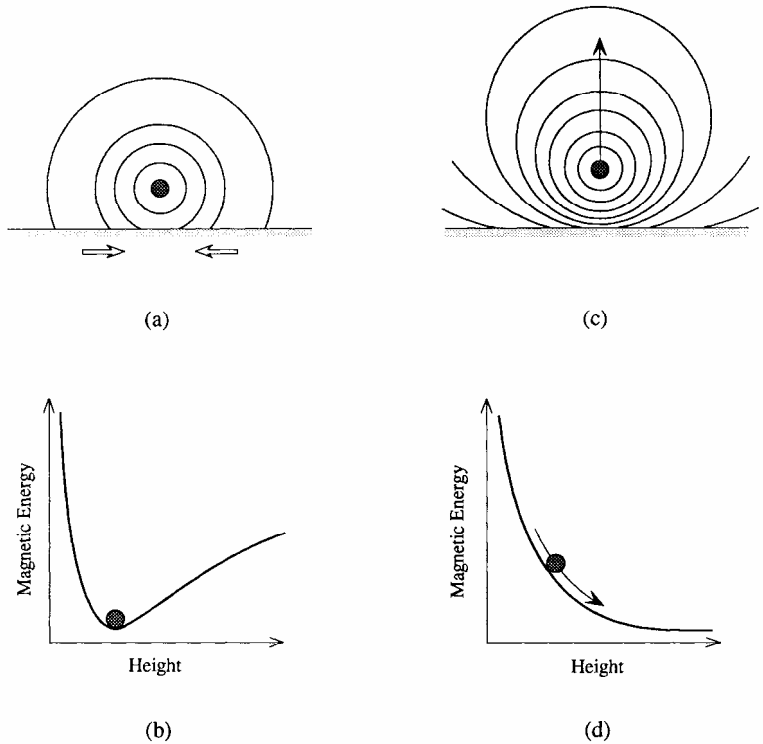

Flux Rope Catastrophe Model

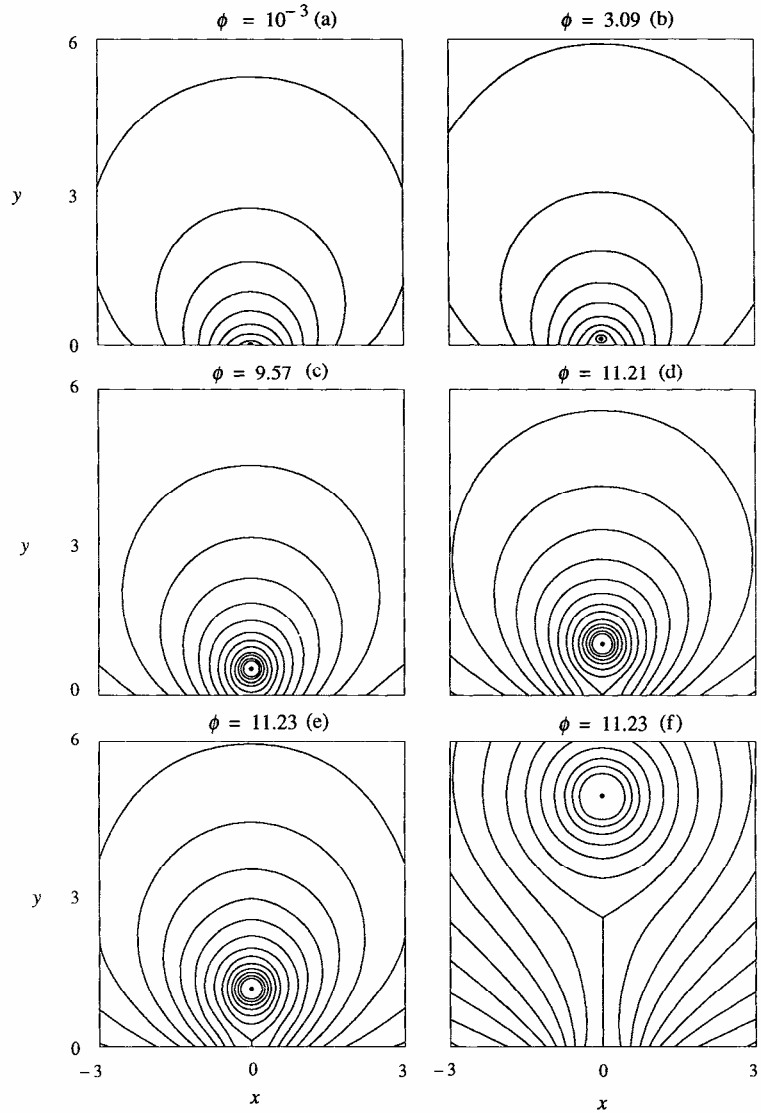

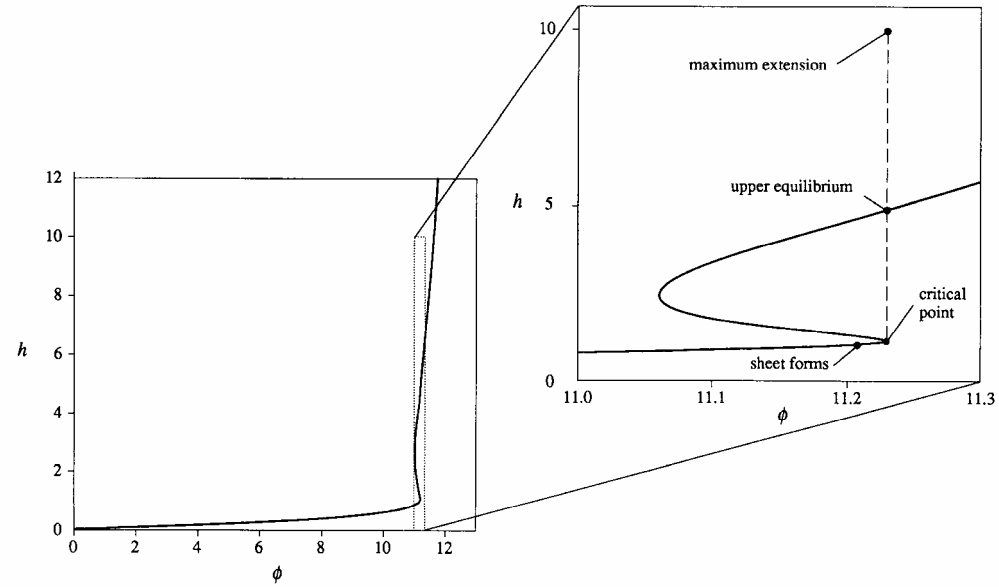

- Flux cancellation should be observed (tether cutting).
- Formation of a current sheet of a finite length may look like field opening.
- Reconnection is required to further expel the flux rope.

Current Driven Instability of Flux Ropes

(Chen, 1989)

Assumptions

- Coronal current is closed beneath the solar surface.
- Coronal current is governed by the subsurface condition.
- The solar surface is not a rigid perfect conductor, but it can respond to the coronal evolution.

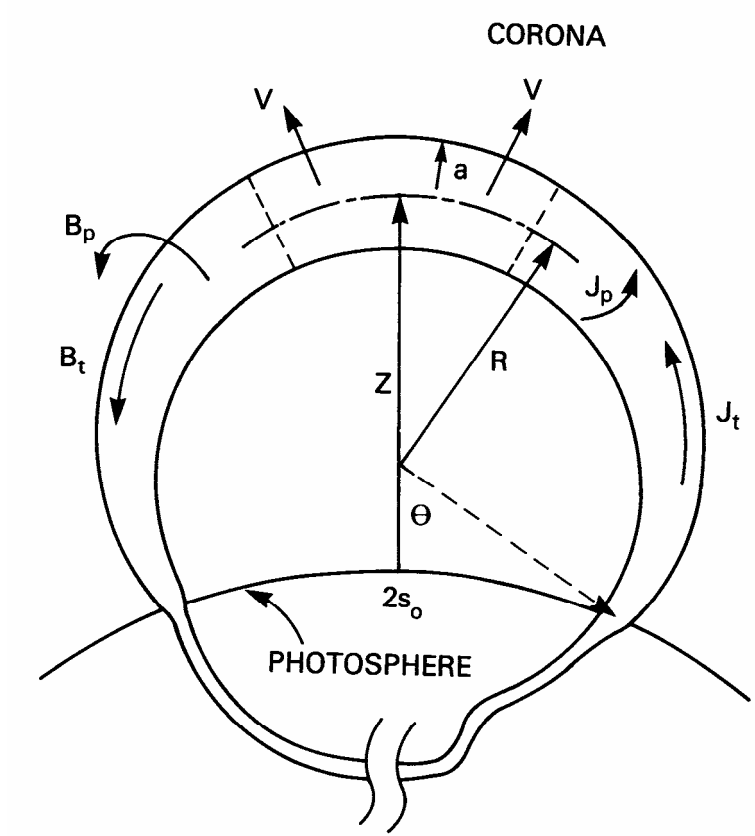

For a strong enough toroidal current, the flux rope is unstable to radial expansion.

Comparison of Two Flux Rope Models

Forbes	Chen
• Photospheric inductance infinite	• Photospheric inductance finite
• Poloidal flux of the flux rope increased by flux cancellation	• Flux rope poloidal flux injected from below the surface
• Ignorable photospheric motion during eruption	• Measurable photospheric motions (horizontal and/or vertical) during eruption

Ejection of Self-closed Field Structures

(Gibson and Low 1998)

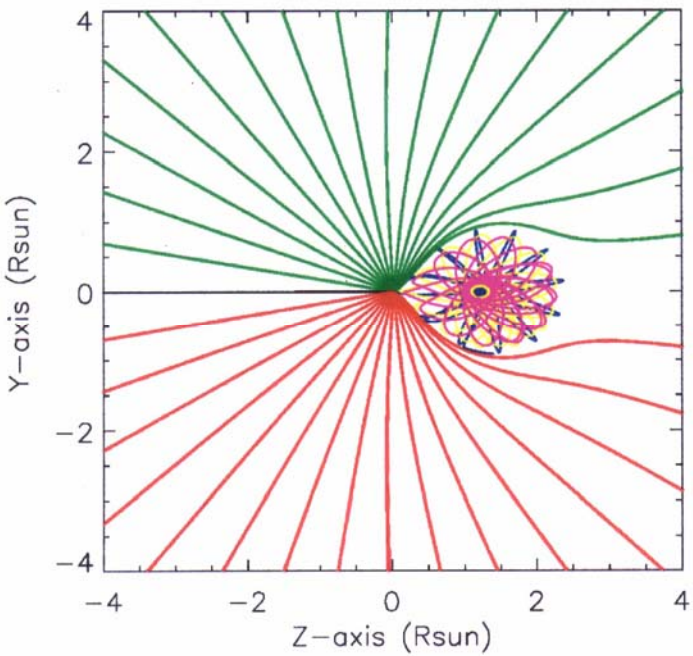

- A self-closed field structure similar to a torus is embedded in an open field and pinned down at one point.

- It expands in a self-similar manner.

Ejection of Self-closed Field Structures

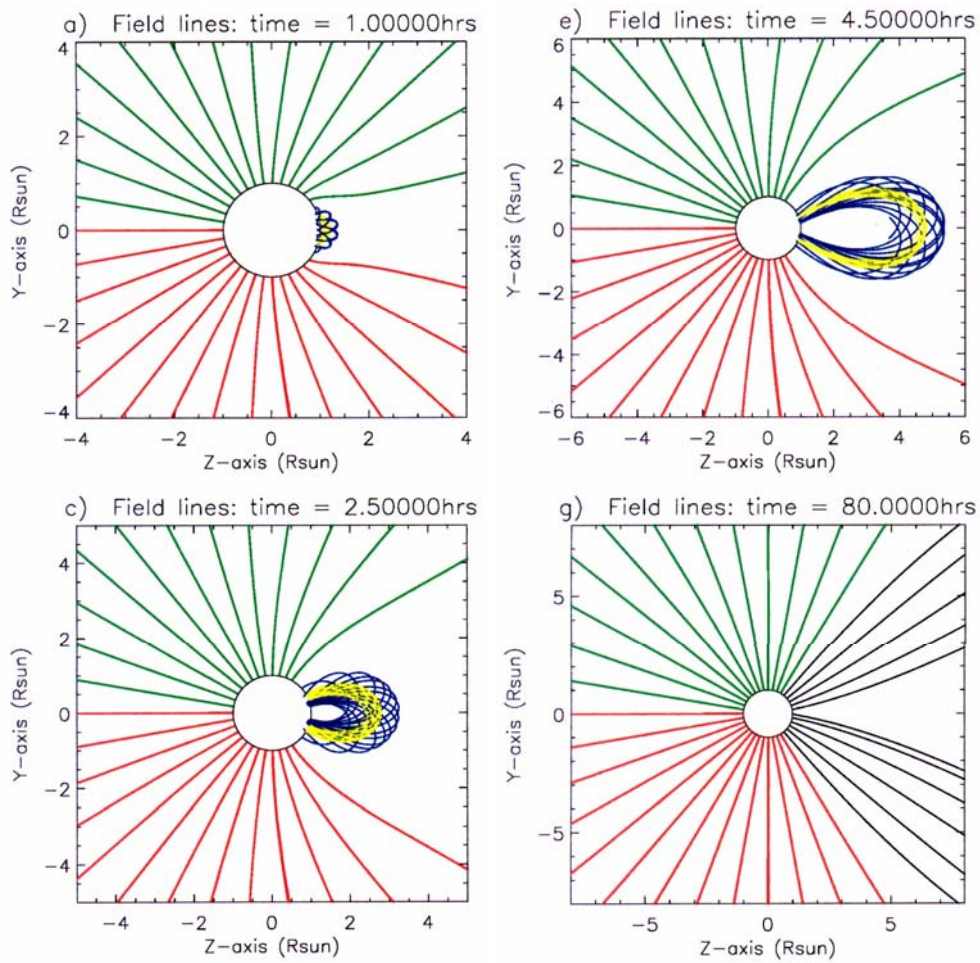

- Inertia-dominant solar interior is not considered.
- Photospheric field (both vertical and horizontal components) changes a lot during eruption.

Development of the A-S Theorem

Aly's conjecture (1984)

Aly found that

$E_{\text{fff}} < E_{\text{UB}} < \infty$

where E_{UB} depends on B_n only.

If $E_{\text{LUB}} \equiv \sup E(\mathbf{B}_{\text{fff}})$ is also dependent on B_n only,

$E_{\text{LUB}} = E_{\text{open}}$?

Proofs by Aly (1991) and Sturrock (1991)

Under footpoint motions conserving

B_n and field connectivity,

$$\delta E = -(1/4\pi)\int_S B_n(\boldsymbol{\delta}\mathbf{x}_\mathbf{t} \bullet \mathbf{B}_\mathbf{t})\, dS$$

can always be made positive by choosing a right $\boldsymbol{\delta}\mathbf{x}_\mathbf{t}$.

$\delta E = 0$ for any footpoint motions,

iff $\mathbf{J} = 0$ or $B_n = 0$ at the boundary, *i.e.*,

for potential fields or the open field.

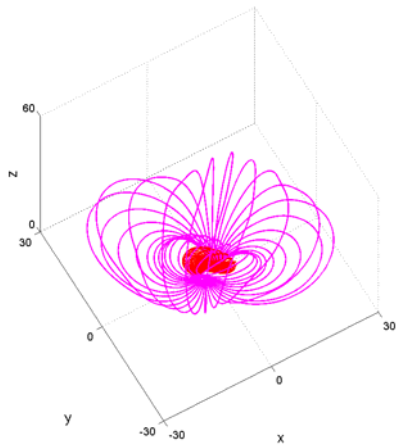

If the maximum energy state $\mathbf{B}+$ exists, $\delta E = 0$ for $\mathbf{B}+$.

Since $E_{\text{open}} > E_{\text{potential}}$,

$\mathbf{B}+ = \mathbf{B}_{\text{open}}$ and $E_{\text{potential}} \le E_{\text{fff}} \le E_{\text{open}}$.

Important Assumptions Conditioning Aly and Sturrock's Proofs

1. There should be an energy-increasing sequence of FFFs converging to a stationary state $\mathbf{B}_\infty$, for which $\delta E = 0$.

2. If $\mathbf{B}_\infty$ exists, it should also hold that $E(\mathbf{B}_\infty) = E_{\mathrm{LUB}}$.

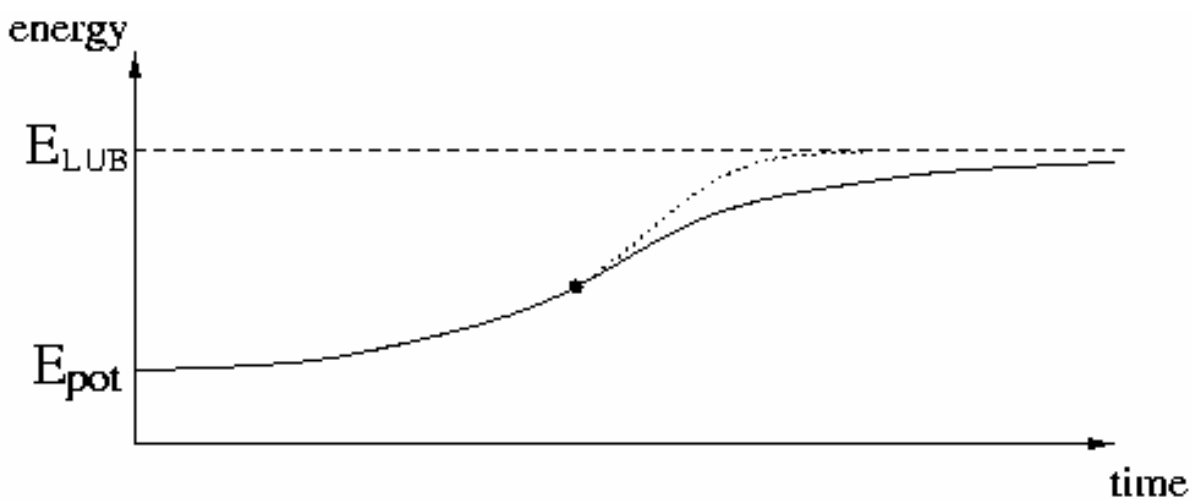

These assumptions cannot be taken for granted!

Are proofs by Aly and Sturrock complete?

- All energy-increasing sequences may terminate without converging to a stationary state with $\delta E = 0$.
- It is possible that $E(\mathbf{B}_\infty) < E_{\mathrm{LUB}}$.
  Insight can be obtained from the toroidal field energy of 2.5D force-free fields in Cartesian Coordinates.

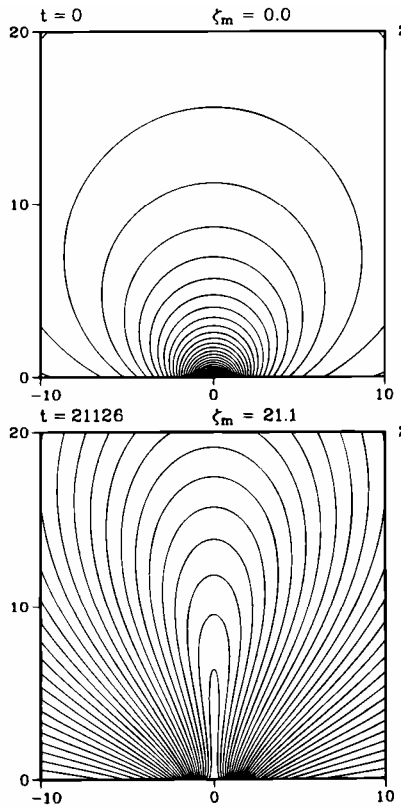

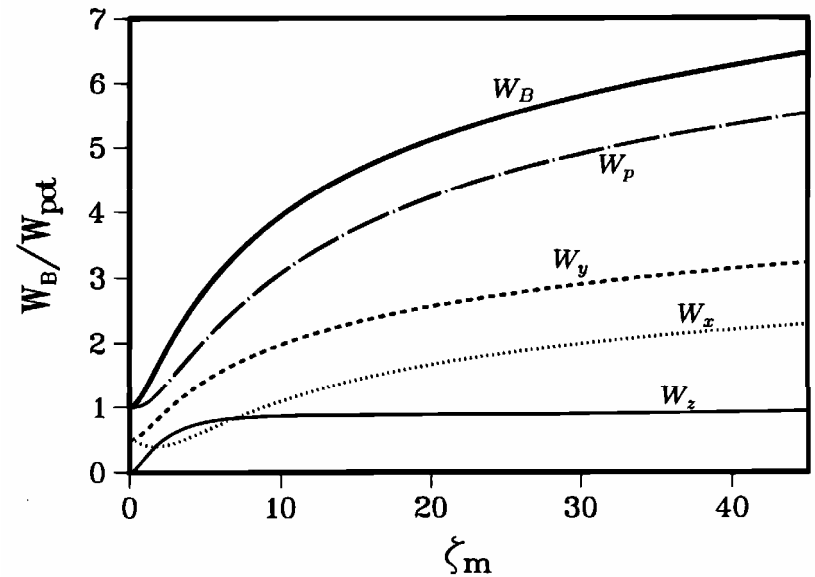

$$\lim_{\zeta\to\infty} \mathbf{B} = \mathbf{B}_{\mathbf{open}}$$

$$\lim_{\zeta\to\infty} W_z = W_{z\,\mathrm{LUB}} \quad \text{but} \quad W_z(\mathbf{B}_{\mathbf{open}}) = 0\,!$$

Convergence of Vector Fields
(special thanks to J. J. Aly)

If $\lim_{k\to\infty} \int_{z>0} |\mathbf{B_k} - \mathbf{B}|^2 \, dV = 0$,

$$\int_{z>0} \mathbf{B}^2 dV = \lim_{k\to\infty} \int_{z>0} \mathbf{B_k}^2 dV .$$

If $\lim_{k\to\infty} \int_{z>0} \mathbf{A} \bullet (\mathbf{B_k} - \mathbf{B})^2 dV = 0$ for any vector field $\mathbf{A}$,

$$\int_{z>0} \mathbf{B}^2 dV \le \lim_{k\to\infty} \int_{z>0} \mathbf{B_k}^2 dV .$$

FFFs Not Governed by the A-S Theorem

The following fields are excluded in Aly's proof.

- Force-free fields containing a flux system that is completely detached from the boundary, such as a magnetic torus.
- Force-free fields containing knotted field lines.

These fields are excluded not because the proof procedure of Aly and Sturrock does not apply to them, but because they are expected not to conform to those assumptions!

Therefore, there can be many other classes of FFFs not governed by the A-S theorem!

We Raise a Question.

Completely detached magnetic flux systems or knotted field lines are unlikely to appear commonly in the solar atmosphere, particularly before eruption.

Are there any FFFs not governed by the A-S theorem, which are considered to be ubiquitous in the sun, and which can be generated by a simple mechanism?

In this study, we pay attention to interwinding multiple flux systems.

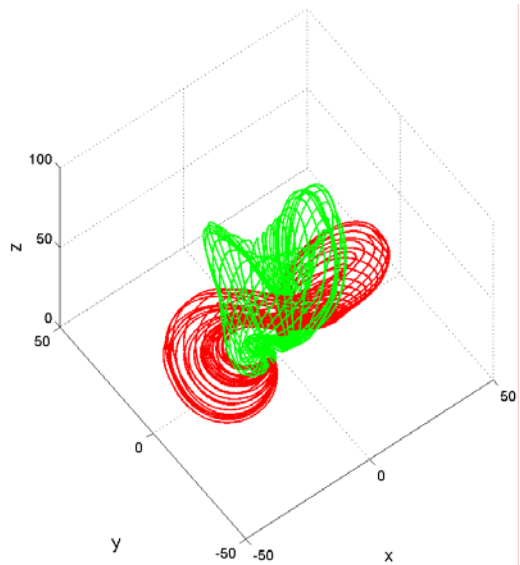

Why Study Interwinding Multiple Flux Systems

1. They are never studied in regard to A-S theorem .

- All previous studies dealt with FFFs in smooth single flux systems.

- Interwinding multiple flux systems generally cannot be generated from potential fields by footpoint motions conserving B_n and field connectivity.

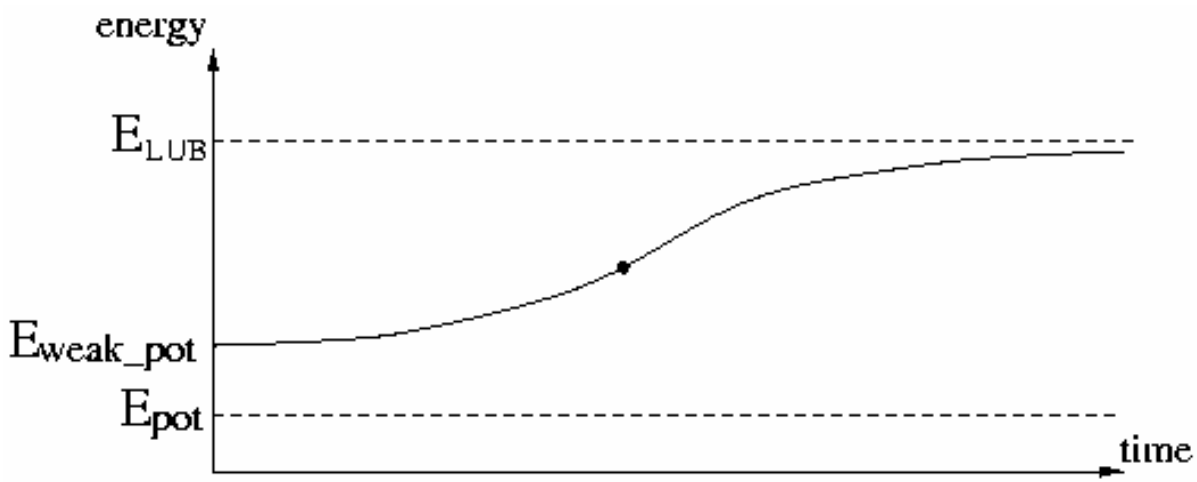

Why study interwinding multiple flux systems

2. They are considered to exist commonly in the sun.

- Subsurface magnetic fields are believed to consist of filamentary flux tubes. After they emerge above the solar surface into the corona, the partitional structure will more or less be retained unless magnetic reconnection totally destroys current sheets.
- In larger scales, flux systems emerging at different times in one location will have little field connectivity among them and will remain separated by current sheets.

Here we study two-flux systems, which are the simplest among multiple flux systems.

Boundary Normal Field Distribution and Field Connectivity (Case 1)

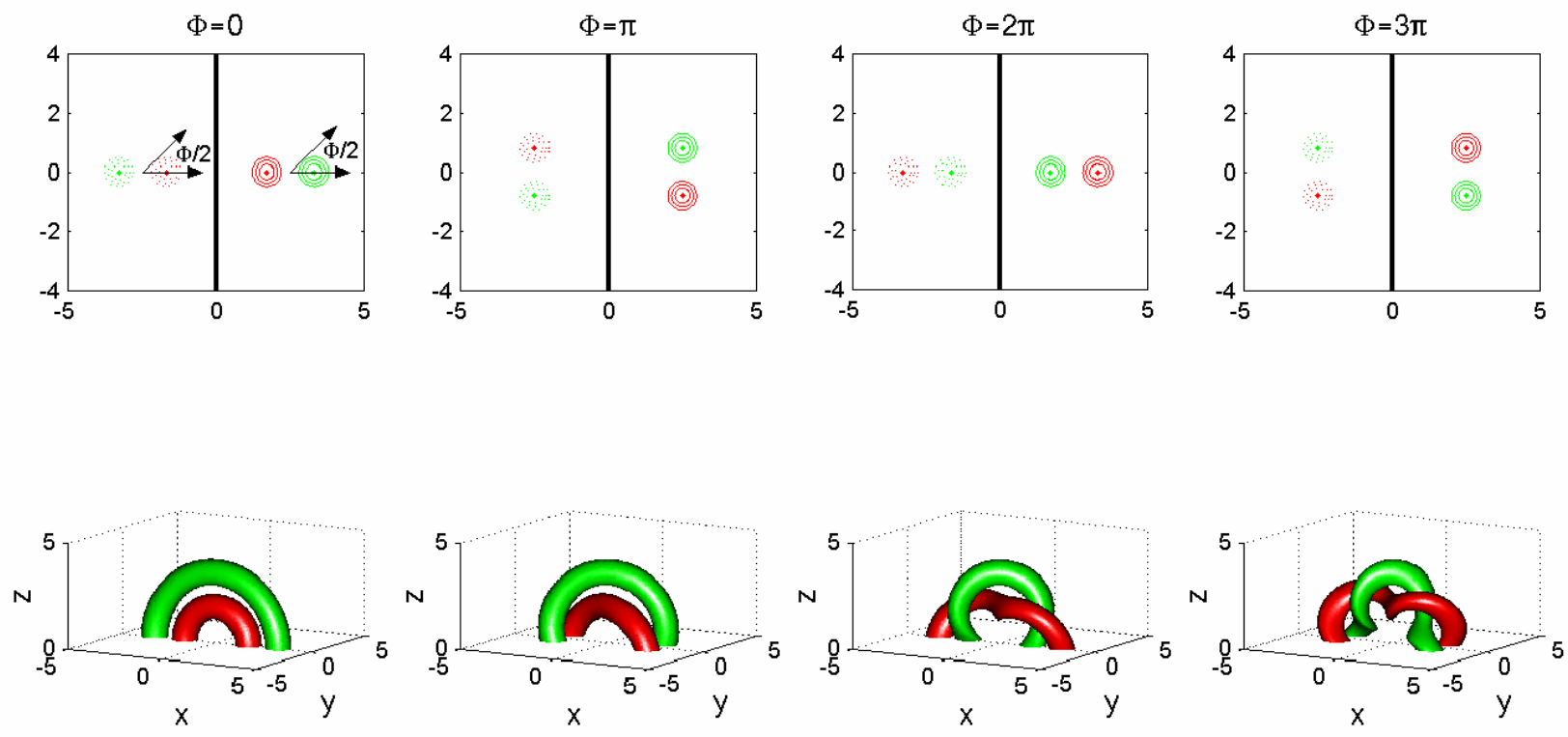

- Upper panels: Magnetograms showing the boundary normal field distribution (solid lines for positive polarity and dotted lines for negative polarity).
- Lower panels: Sketches of field connectivity. In Case 1, the red flux system takes a finite volume while the green flux system takes the infinite rest volume.

Flux Surfaces of the Constructed Force-Free Fields (Case 1)

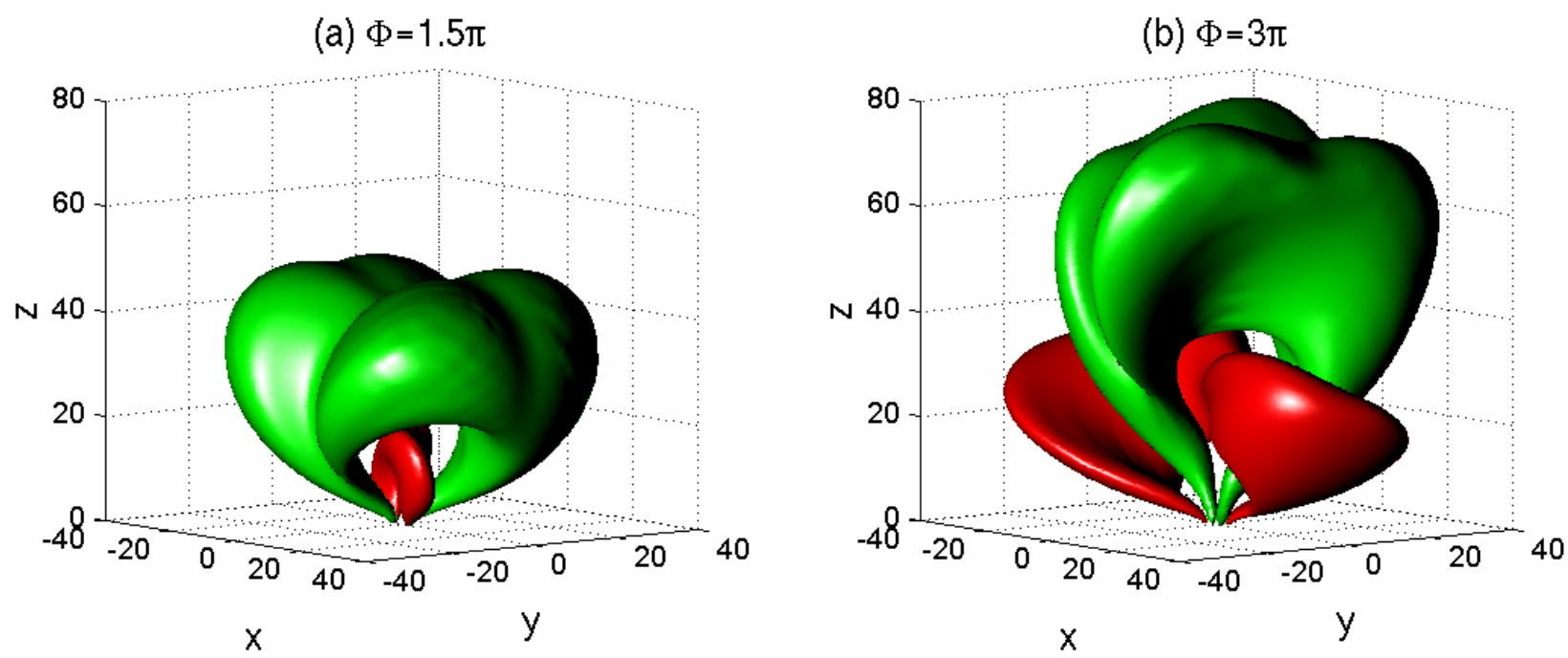

Flux surfaces of the numerically generated force-free fields consisting of two interwinding flux systems (Case 1). Each flux surface contains 25% of the total flux in each flux system.

Energy of Force-Free Fields (Case 1)

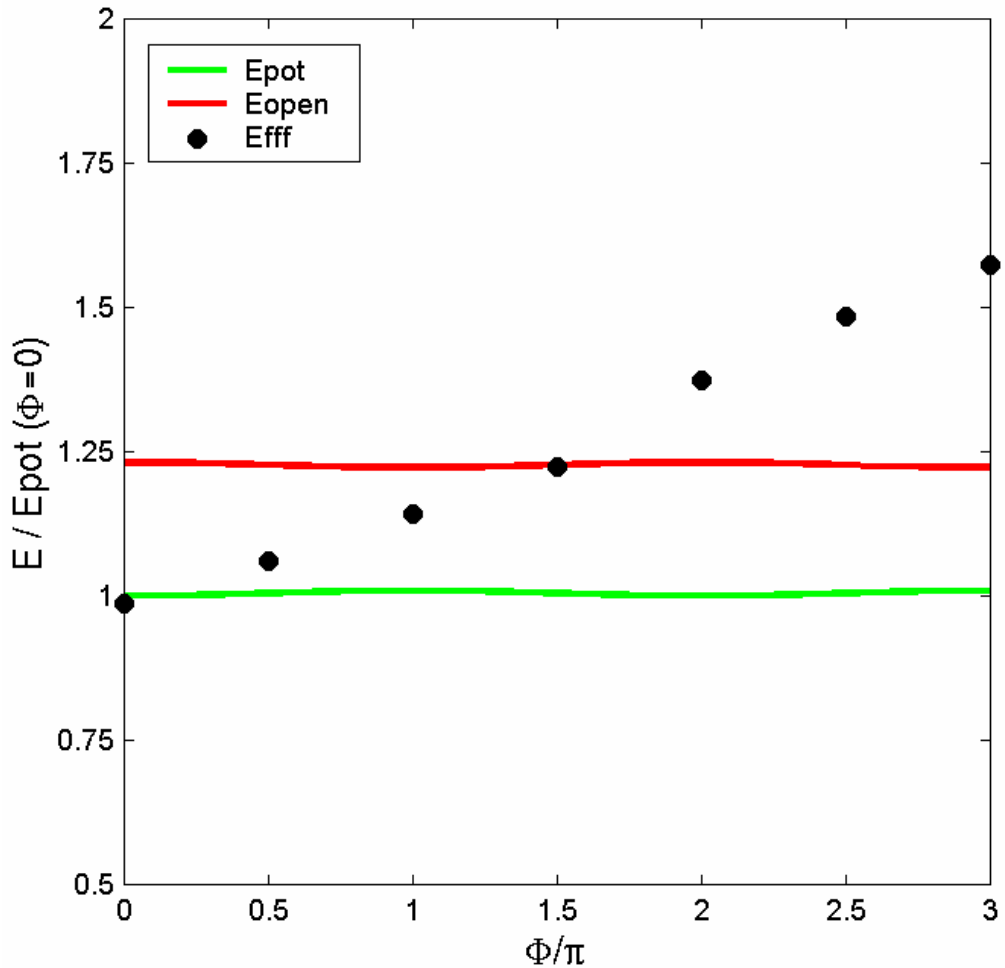

Energy of the numerically generated force-free fields for different winding angles in Case 1. The energies of the potential fields (dashed curve) and of the open fields (solid curve) are also shown as a function of the winding angle.

Boundary Normal Field Distribution and Field Connectivity (Case 2)

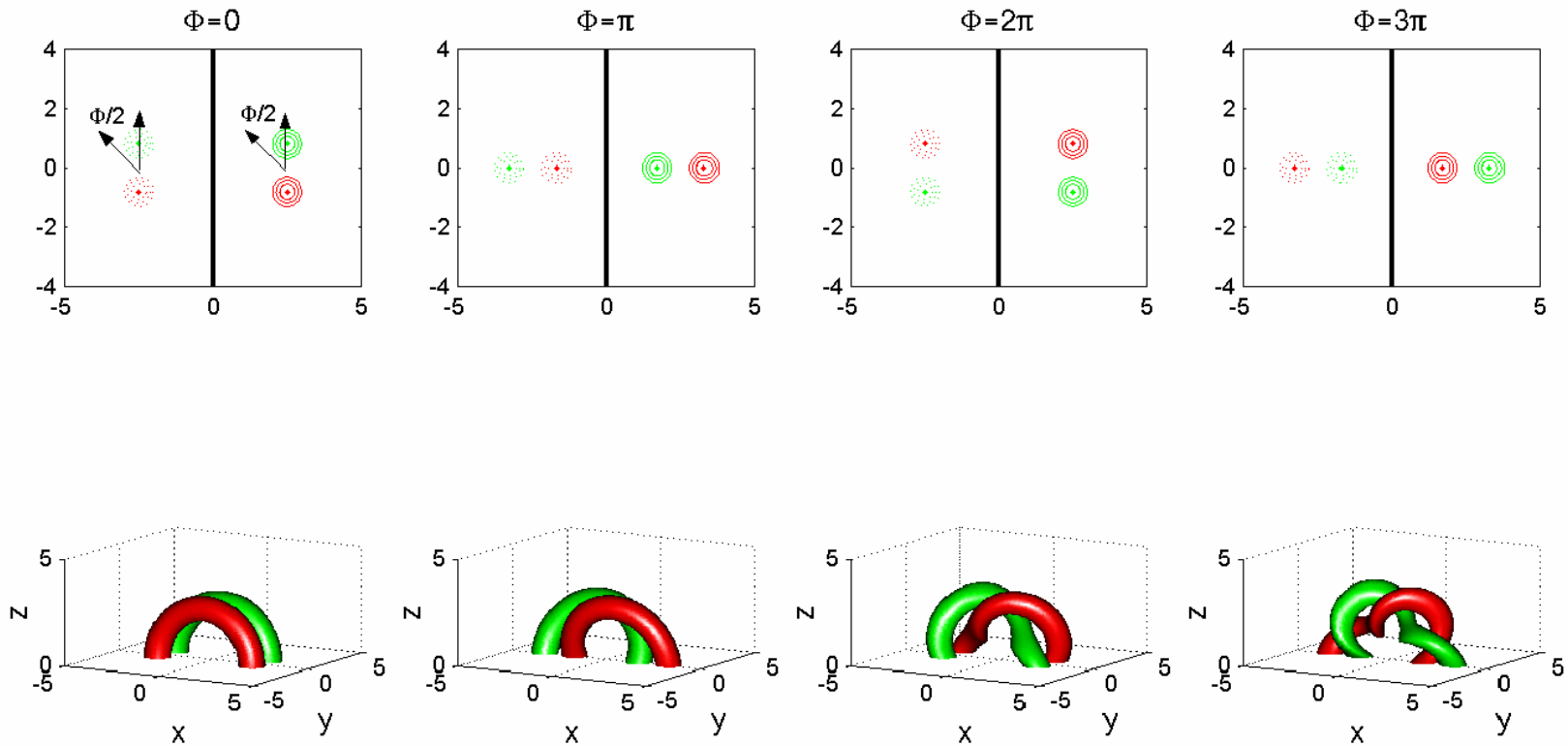

- Upper panels: Magnetograms showing the boundary normal field distribution (solid lines for positive polarity and dotted lines for negative polarity).
- Lower panels: Sketches of field connectivity. In Case 2, both the red and green flux systems take an infinite volume.

Flux Surfaces of the Constructed Force-Free Fields (Case 2)

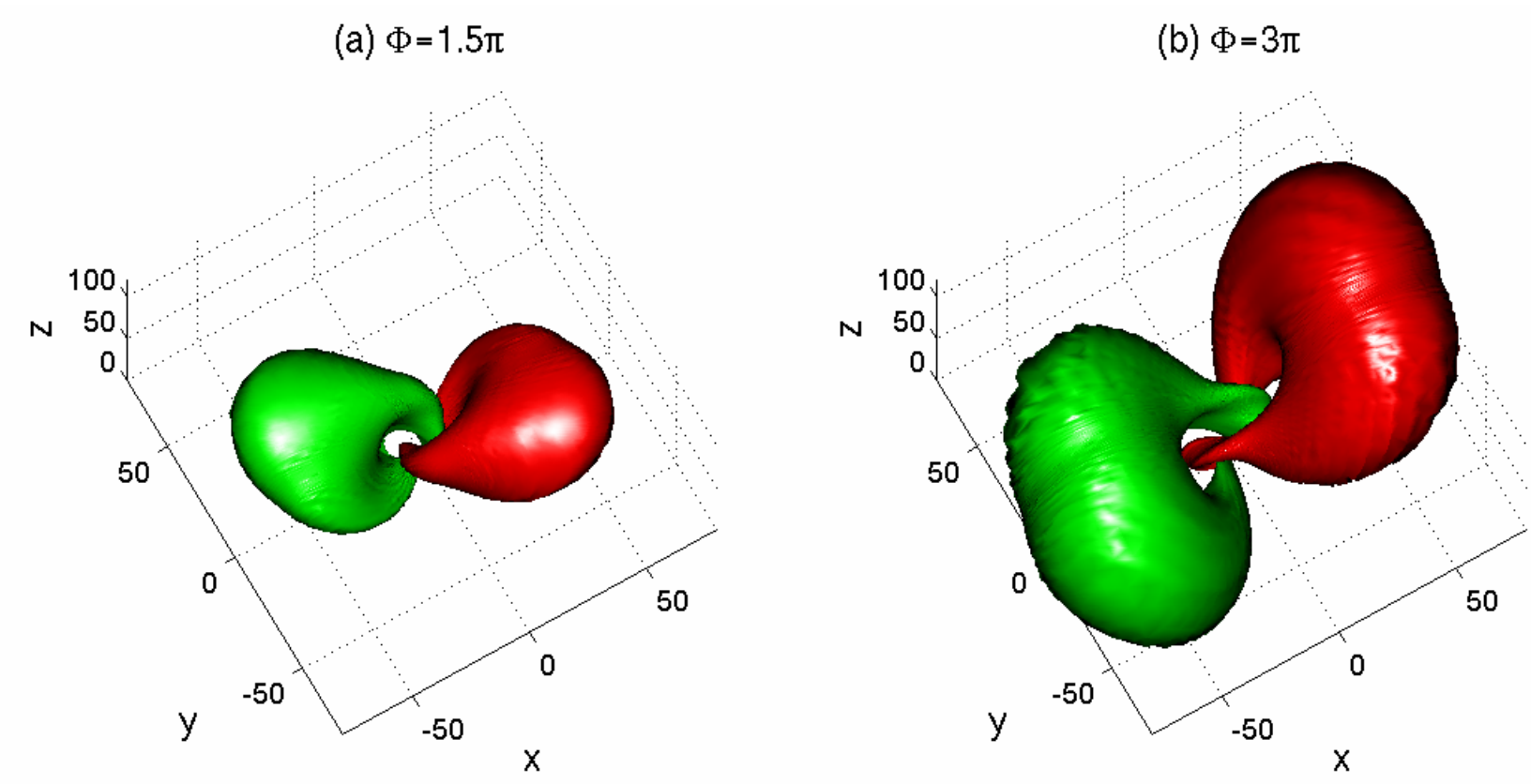

Flux surfaces of the numerically generated force-free fields consisting of two interwinding flux systems (Case 2). Each flux surface contains 25% of the total flux in each flux system.

Energy of Force-Free Fields (Case 2)

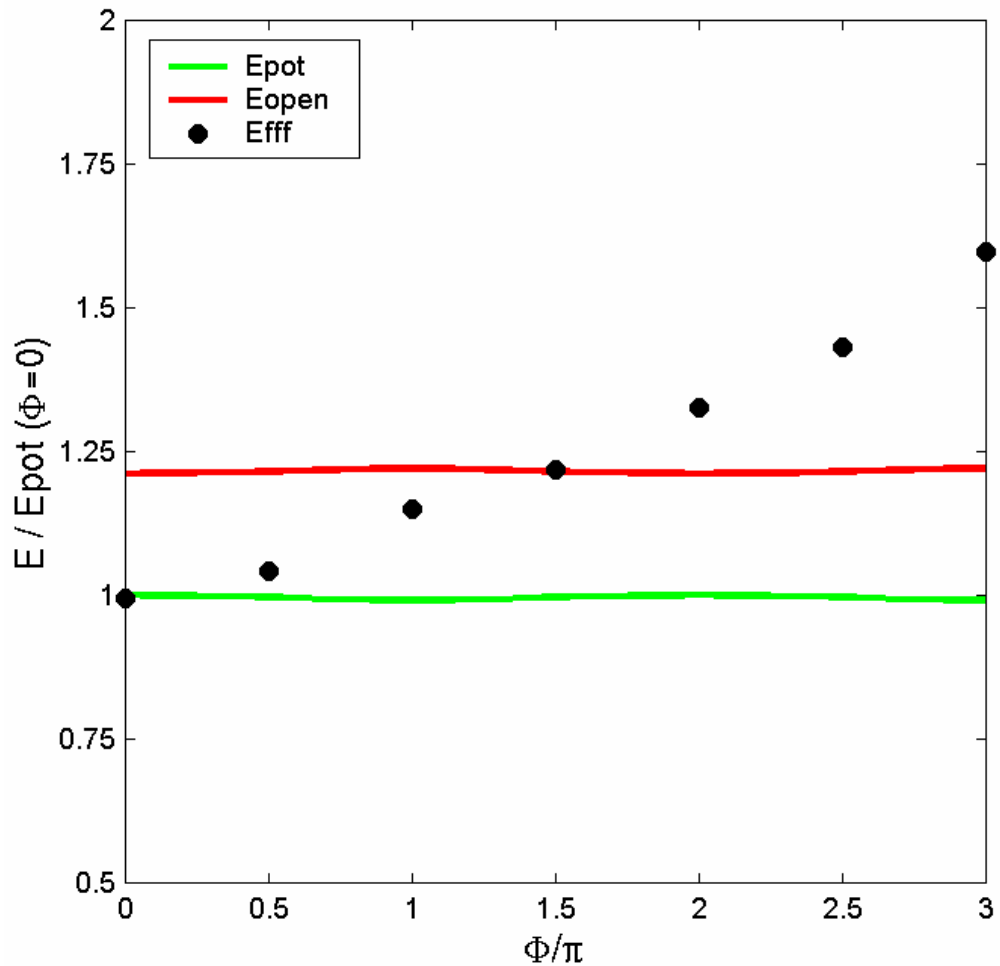

Energy of the numerically generated force-free fields for different winding angles in Case 2. The energies of the potential fields (dashed curve) and of the open fields (solid curve) are also shown as a function of the winding angle.

Will Our Results Be Valid in Systems of an Infinite Size?

1. **An energy upper bound** (not the least upper bound)

$$E_{\mathrm{UB}} = \frac{1}{4\pi}\left(\int_{z=0} B_n^2\, dx\, dy\right)^{\frac{1}{2}}\left(\int_{z=0} r^2 B_n^2\, dx\, dy\right)^{\frac{1}{2}}$$

$$= 10.7\, E_{\mathrm{pot}}(\Phi = 0) = 8.69\, E_{\mathrm{open}}(\Phi = 0) \;>> E_{\mathrm{fff}}$$

2. **Relations holding for infinite size FFF systems**

$$\int_{z=z_0}\left(B_x^2 + B_y^2\right) dx\, dy = \int_{z=z_0} B_z^2\, dx\, dy \qquad (2.1)$$

$$\frac{1}{8\pi}\int_{z>z_0} B^2\, dx\, dy\, dz = \frac{1}{4\pi}\int_{z>z_0}(xB_x + yB_y)B_z\, dx\, dy \qquad (2.2)$$

Discrepancies between the RHS and LHS are < 3% for (2.1) and <9% for (2.2)

Will our results be valid in systems of an infinite size? - continued

3. Different computational box sizes

$$E_{160} : 160 \times 160 \times 160$$

$$E_{300} : 300 \times 300 \times 300$$

$$E_{400} : 400 \times 400 \times 400$$

$$(E_{160} - E_{300}) / E_{300} < 0.05$$

$$(E_{300} - E_{400}) / E_{400} < 0.014$$

Energy roughly varies with the box size L $(= V^{\frac{1}{3}})$ as

$$E_L \sim E_\infty + c/L \text{ for large } L$$

$$\Rightarrow 0.95\, E_{400} < E_\infty < E_{400}$$

We are convinced that some of our force-free fields really have more energy than the open field energy.

Features to Be Compared with Observations

Case 1 $\Phi = 2\pi$

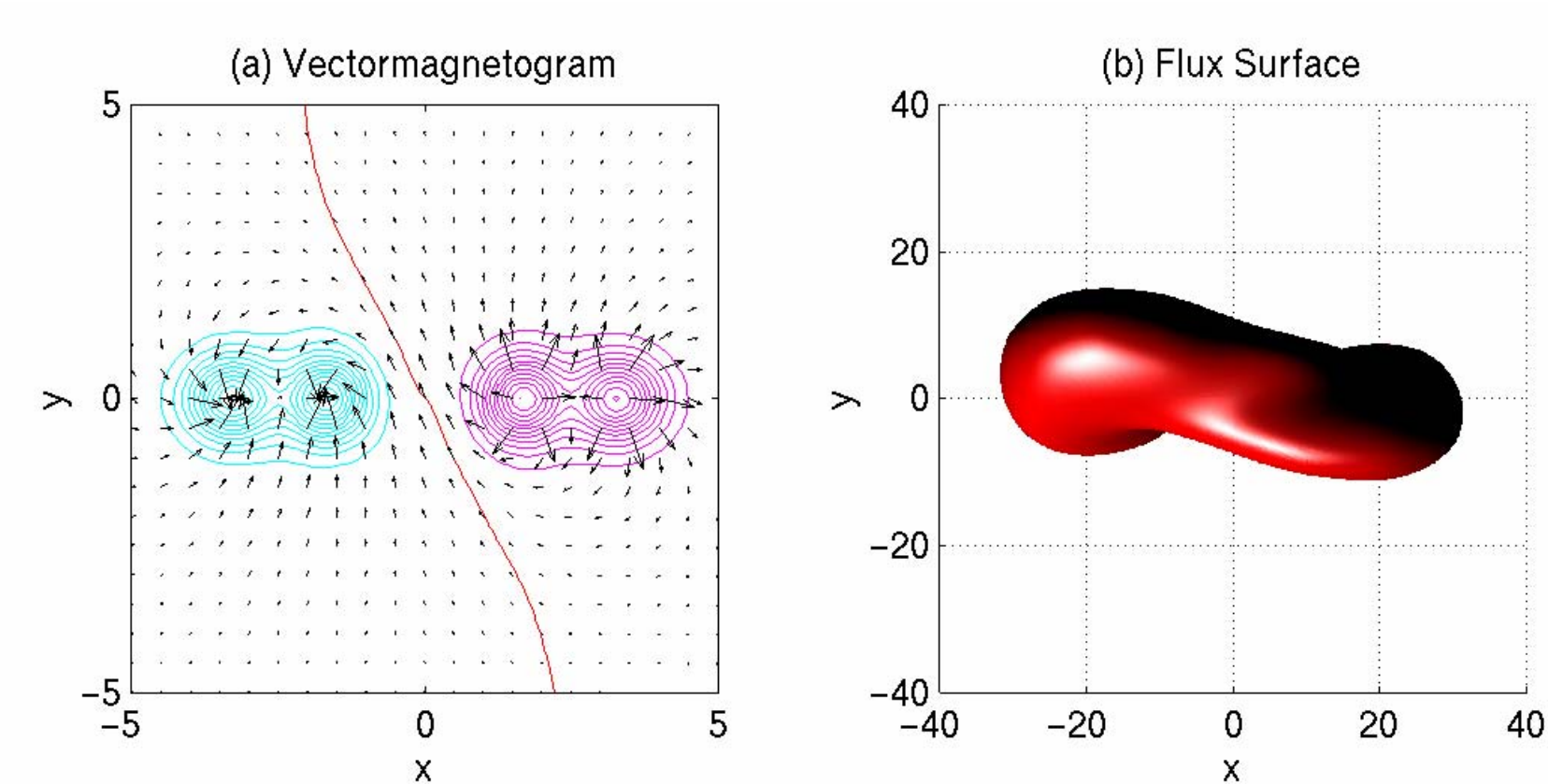

(a) Vector magnetogram generated from our FFF solution at the height $z = 0.22$.

(b) Projected image of a flux surface containing 95% of the total flux of the inner (red) flux tube.

Features to Be Compared with Observations

Case 1 $\Phi = 2.5\pi$

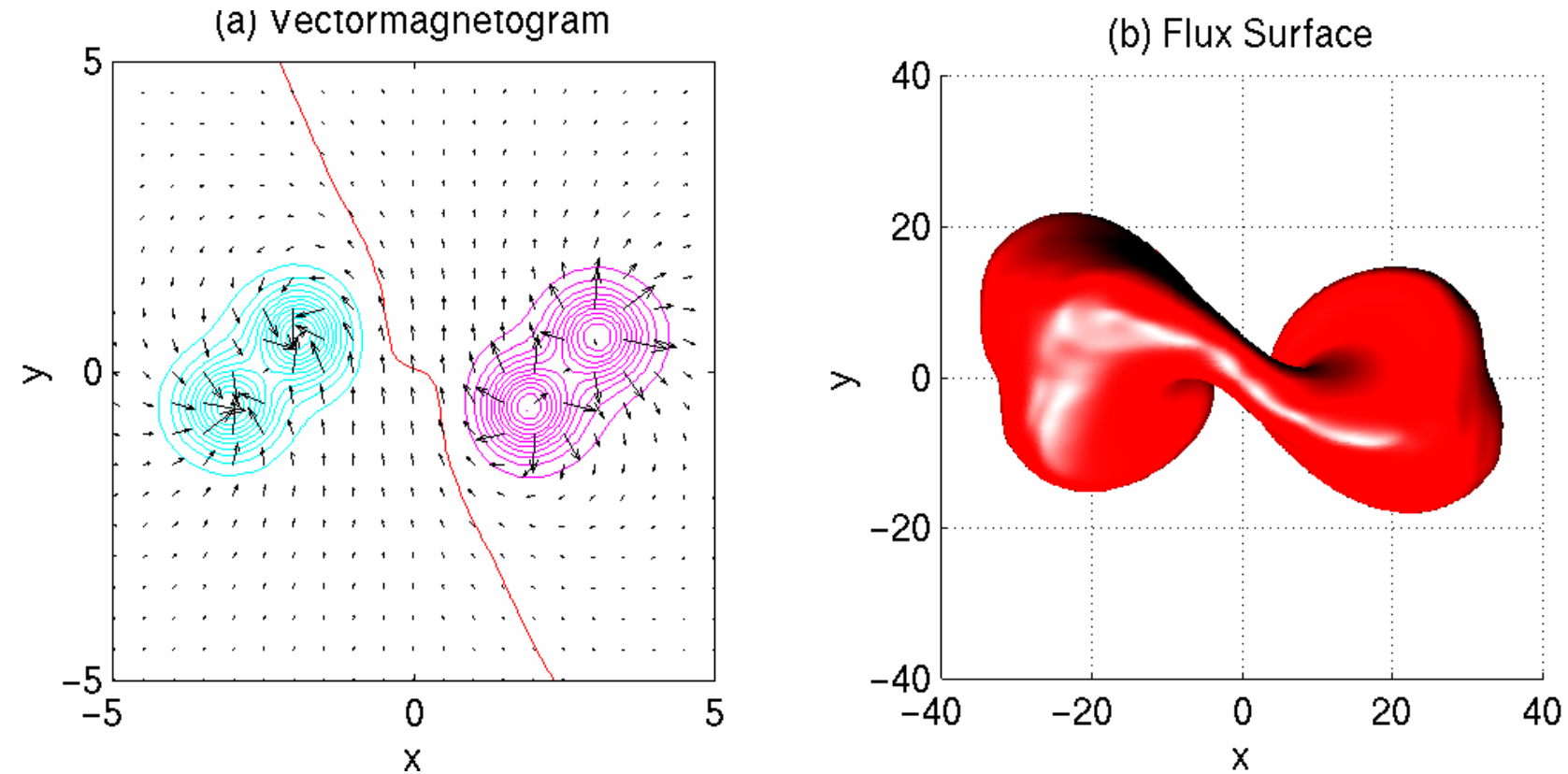

- The magnetic shear increases and the polarity inversion line is more and more tilted with the increasing winding angle.
- The projected flux surface image takes an inverse S-shape resembling a sigmoid.

Observation of Sigmoids

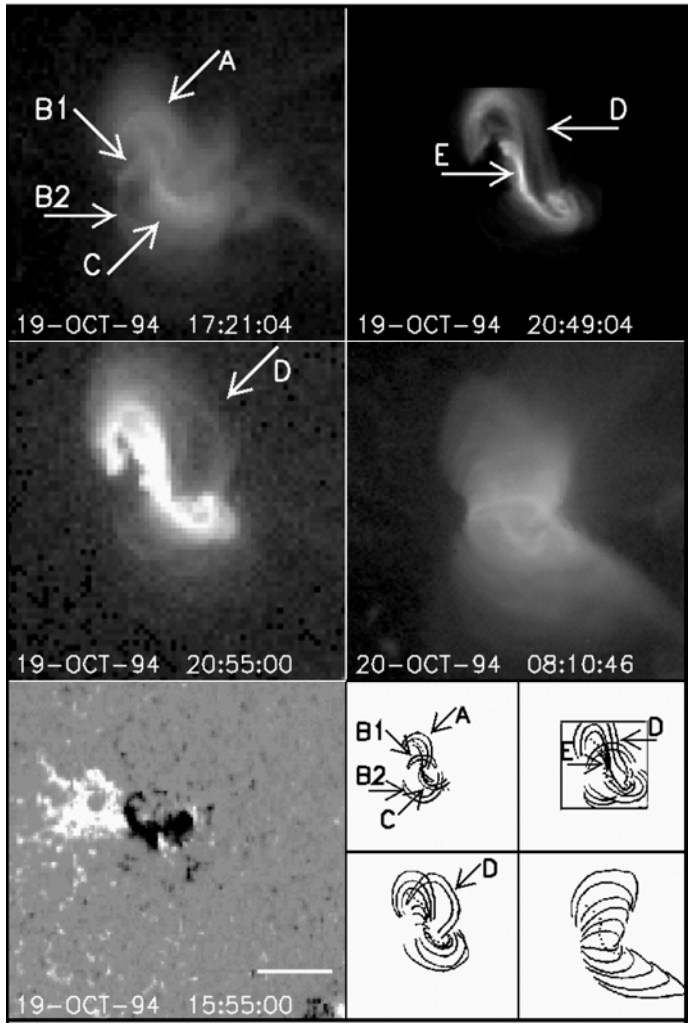

Moore et al. 2001

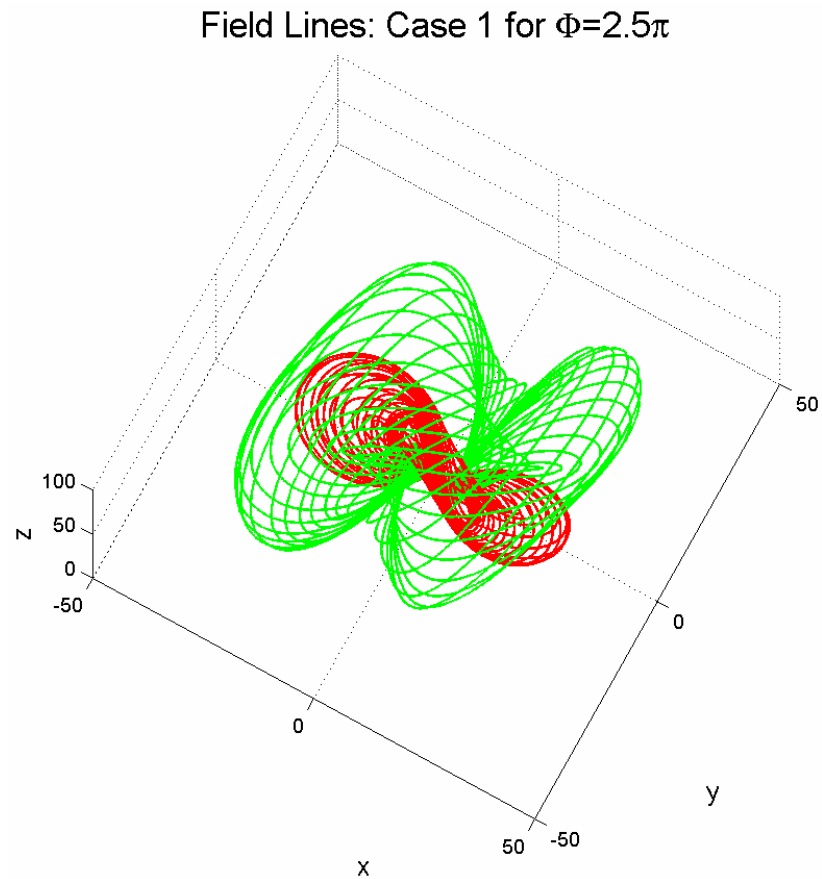

Eruption takes place for

$2\pi \leq \Phi \leq 2.5\pi$

Speculation on Reconnection (Case 1)

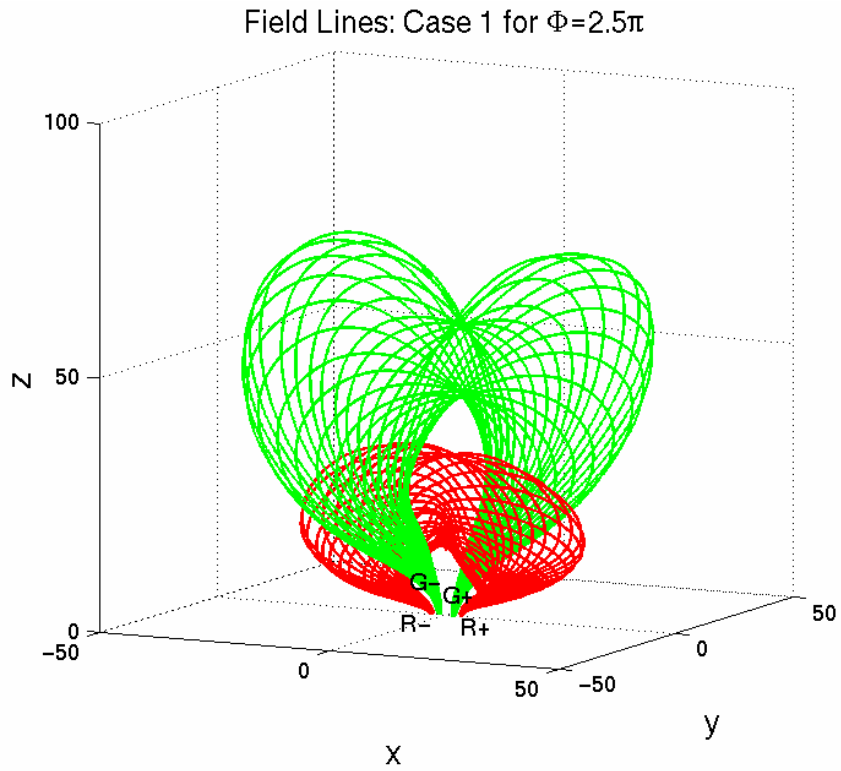

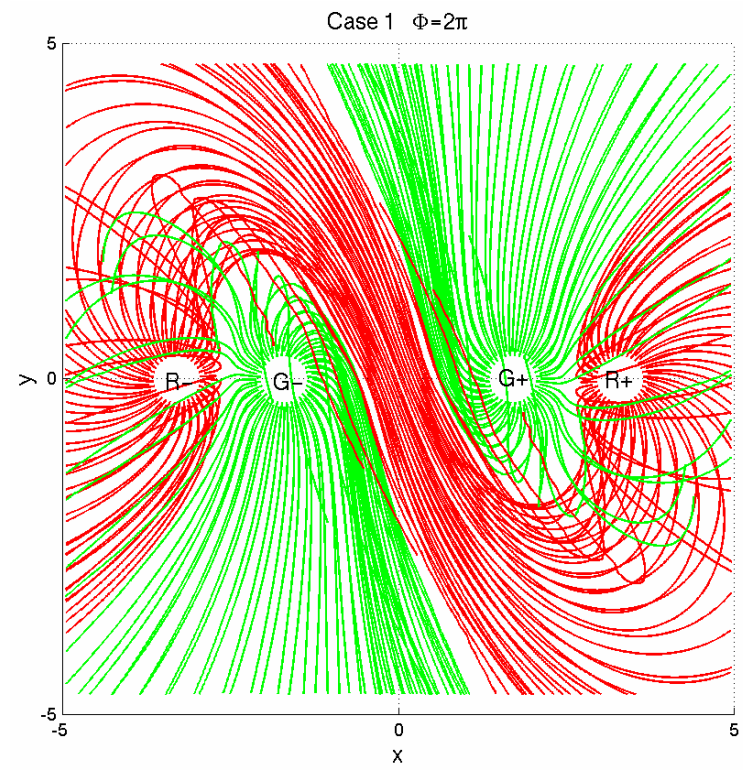

- Reconnection is most likely to occur between G- and G+.
- It will create a huge flux rope wrapping around another.
- Flux cancellation can be expected to be observed.

Features to Be Compared with Observations

Case 2 $\Phi = 2\pi$

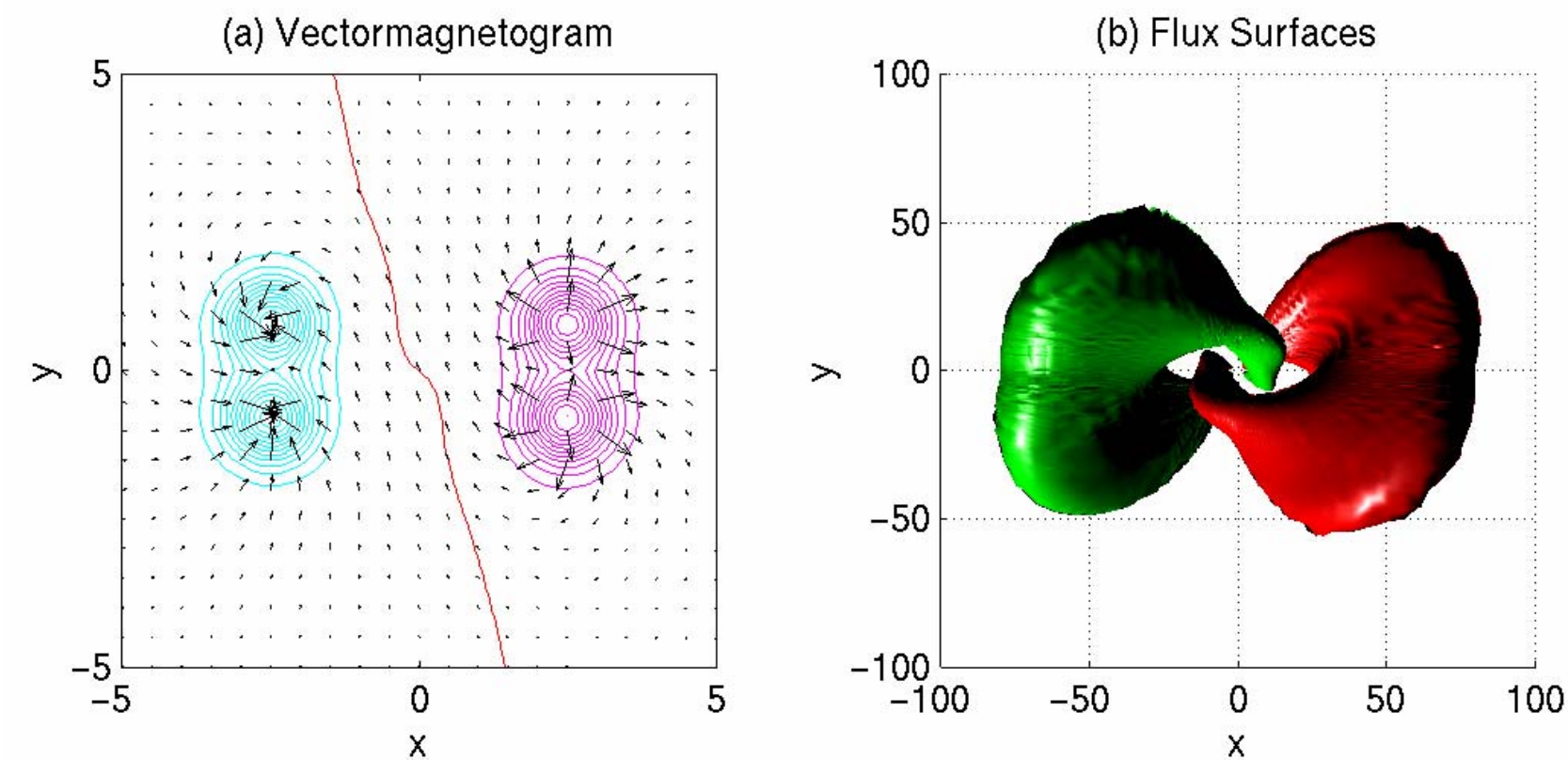

(a) Vector magnetogram generated from our FFF solution at the height $z = 0.22$.

(b) Projected image of flux surfaces containing 20% of the total flux of each flux tube.

Features to Be Compared with Observations

Case 2 $\Phi = 2.5\pi$

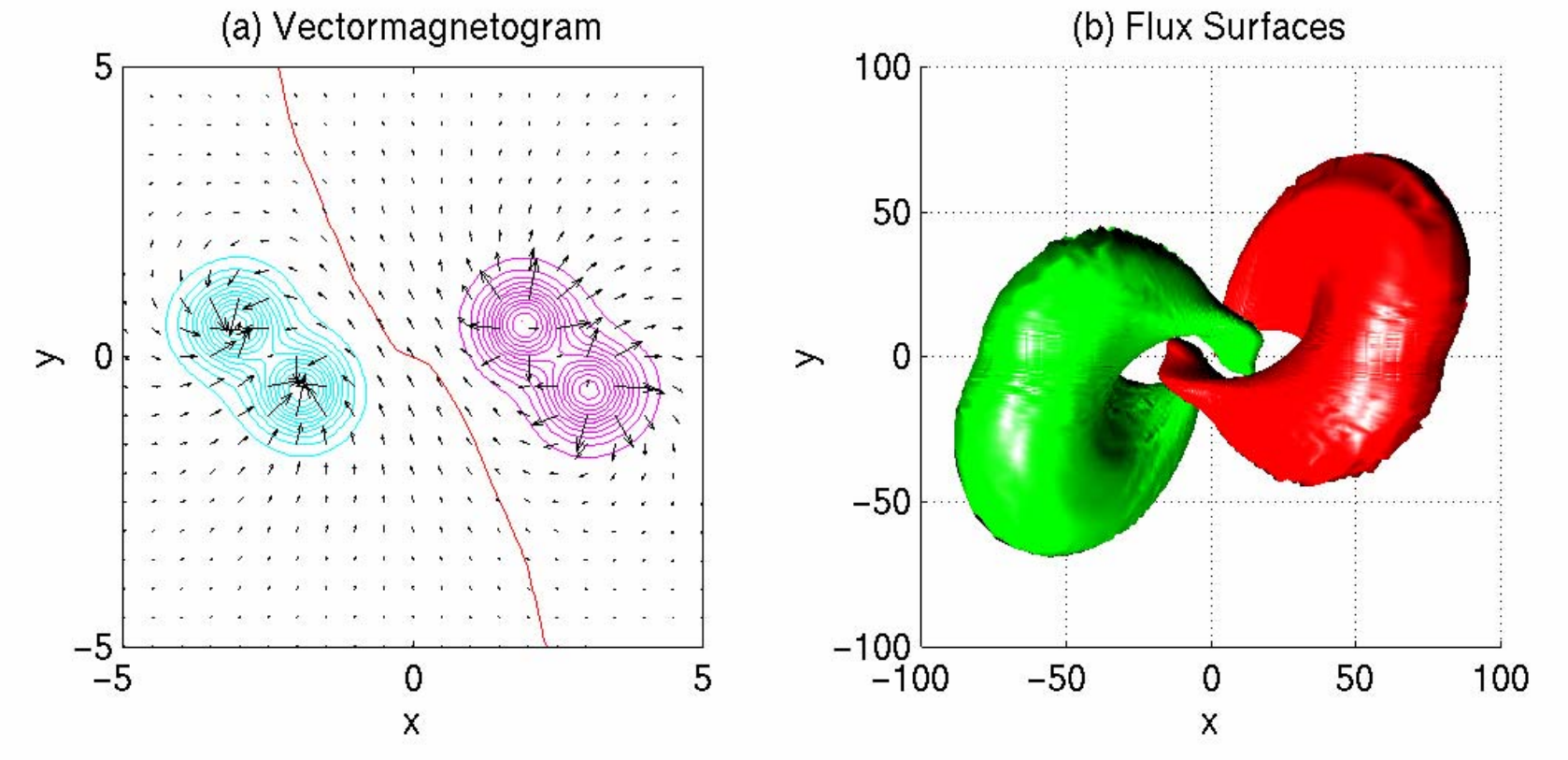

- The magnetic shear increases and the polarity inversion line is more and more tilted with the increasing winding angle.
- The projected flux surface image takes an inverse S-shape resembling a sigmoid.

Observation of Sigmoids

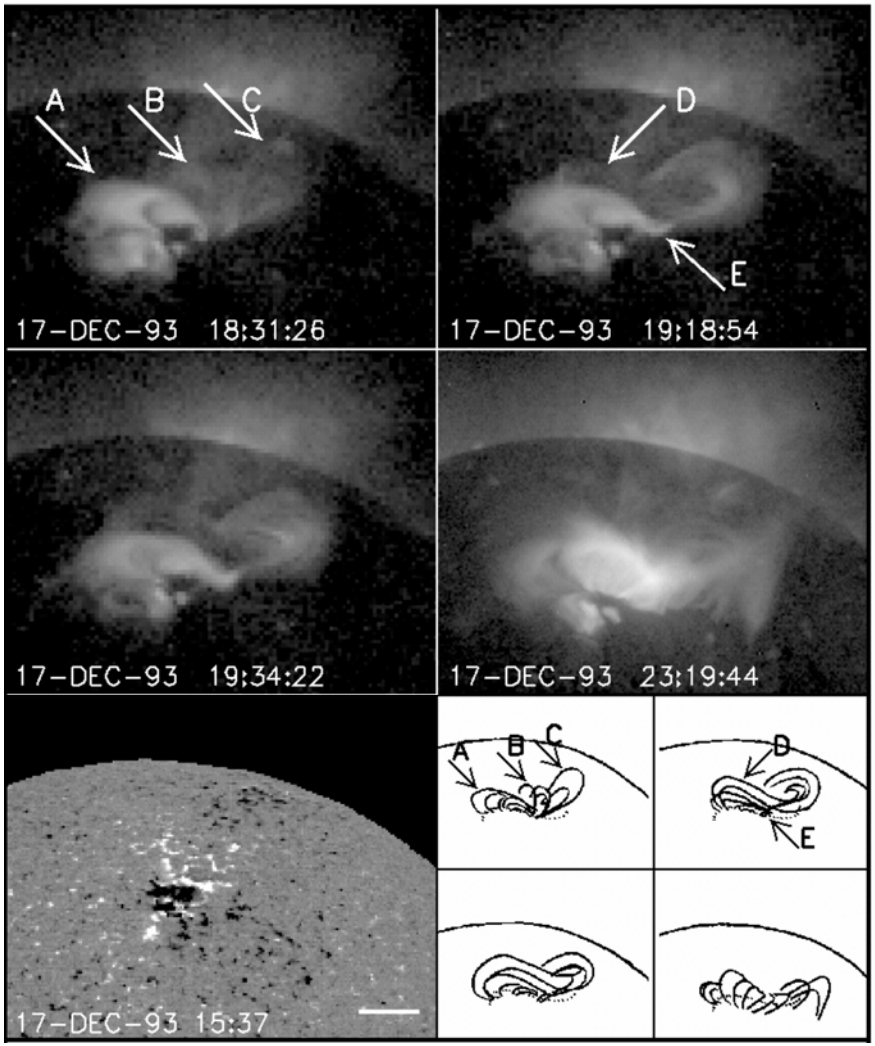

Moore et al. 2001

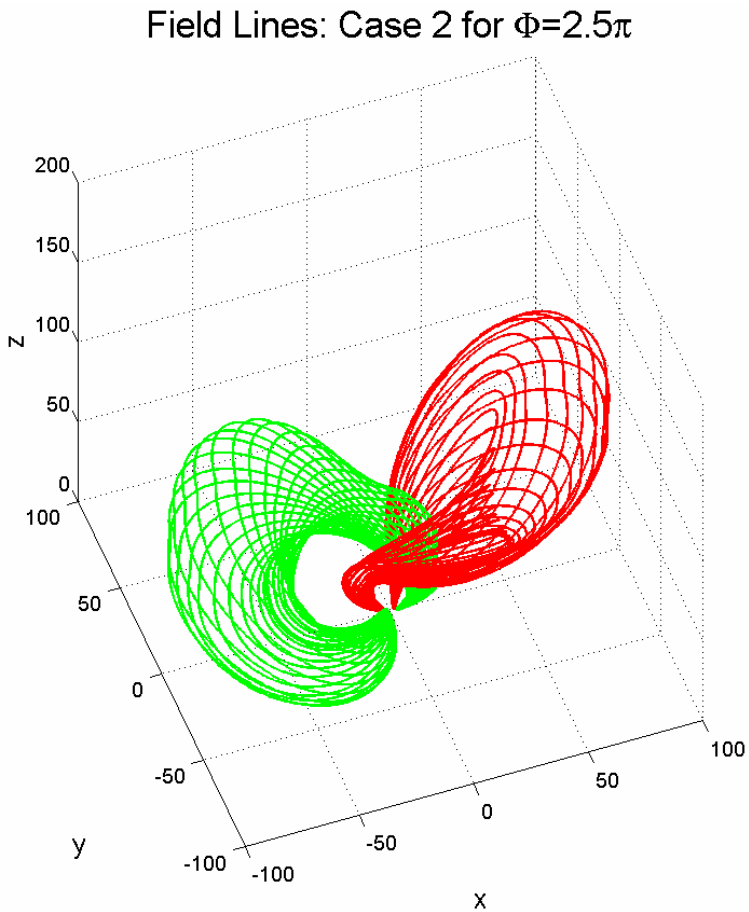

Eruption takes place for

$2\pi \leq \Phi \leq 2.5\pi$

Speculation on Reconnection (Case 2)

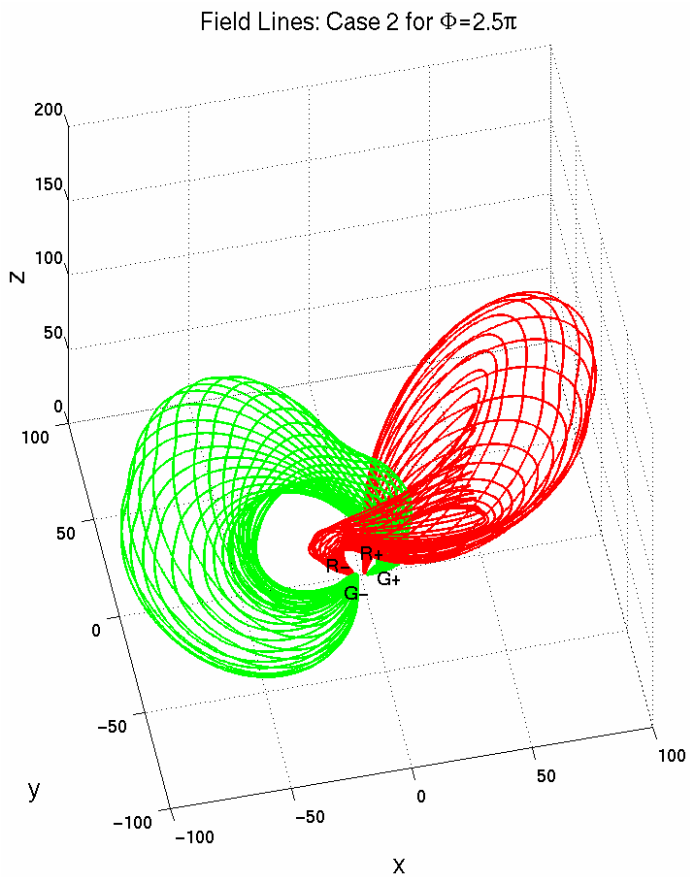

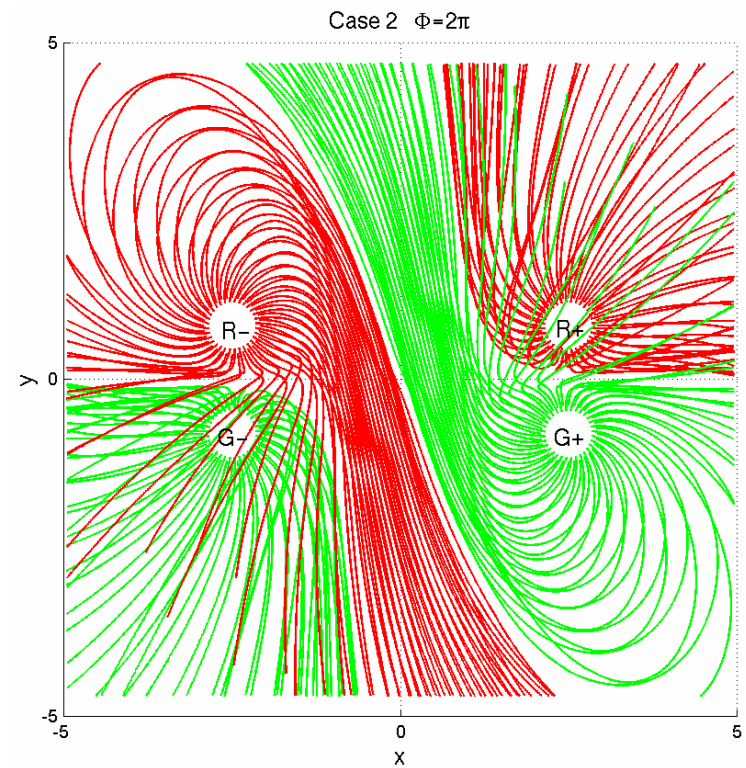

- Reconnection is most likely to occur between R- and G+.
- It will create a long, highly writhed flux rope over an underlying arcade.
- Flux cancellation can be expected to be observed.

What would be the process leading to eruption?

- **Without magnetic reconnection**

  Global non-equilibrium with further winding or twist?
  ⇨ CME with field opening

- **Via magnetic reconnection**

  1. Global non-equilibrium in a new field topology?
     ⇨ CME with field opening
  2. Huge increase of flux volume in new equilibria?
     ⇨ CME with sudden loop expansion, but without real field opening (only apparent field opening)
  3. Sudden energy release with little flux volume change?
     ⇨ Only flares, no CMEs

Conclusion

- There is a class of force-free fields that can have more energy than the open fields.
- These force-free fields belong to multiple flux systems with current sheets, and they can be generated from potential fields by certain footpoint motions that do not conserve the boundary normal field distribution.
- The constructed force-free fields show several features of observed CME-bearing active regions: high magnetic shear, tilted polarity inversion lines and S- (or inverse S-) shaped field structures.

Setup of Numerical Experiment

1. Configurations before interwinding

The boundary normal field distribution:

$$B_n(x,y) = B_z(x,y,0) = \sum_i B_{zi}(\rho_i)$$

$$B_{zi}(\rho_i) = \begin{cases} \pm[1-(\rho_i/R)^2]^2 & \text{if } \rho_i \le R \\ 0 & \text{if } \rho_i > R \end{cases}$$

$$\rho_i = |\mathbf{r} - \mathbf{r}_i|, \quad R = 0.7, \quad i = a_+, a_-, b_+, b_-$$

$$\mathbf{r}_{a\pm} = (\pm 1.7, 0, 0), \qquad \mathbf{r}_{b\pm} = (\pm 3.3, 0, 0) \qquad \text{Case 1}$$

$$\mathbf{r}_{a\pm} = (\pm 2.5, -0.8, 0), \quad \mathbf{r}_{b\pm} = (\pm 2.5, 0.8, 0) \qquad \text{Case 2}$$

The field connectivity of the potential fields for $\Phi = 0$:

$$x_{0+} = -x_{0-}, \quad y_{0+} = y_{0-}$$

(x_{0+}, y_{0+}) and (x_{0-}, y_{0-}): coordinates of conjugate footpoints

Setup of numerical experiment - continued

2. Interwinding of two flux systems

We impose horizontal boundary motions respectively on each side of the polarity inversion line so that each pair of flux patches undergoes a rotational motion with a constant angular velocity centered at the midpoint of each pair. If we relax the two-flux system to a force-free equilibrium after interwinding by any nonzero twist angle Φ, part of the separatrix between the two flux systems will become a current sheet (tangential discontinuity). The field connectivity of a FFF with $\Phi \neq 0$ is definitely different from that of the potential field for the same $B_n(x, y)$ and cannot be created from the potential field by any footpoint motions conserving $B_n(x, y)$ under the ideal MHD conditions.